PROPELLER-RUDDER INTERACTION DUE TO LOADING AND THICKNESS EFFECTS

S. Tsakonas, et al

Stevens Institute of Technology

Prepared for:

Naval Ship Research and Development Center

September 1972

R-1589

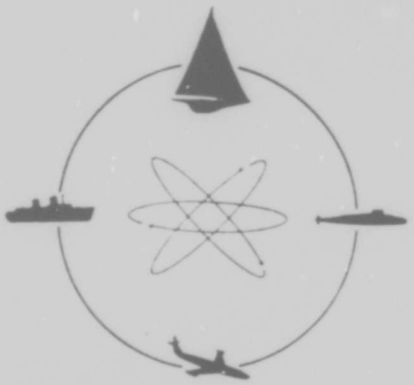

DAVIDSON LABORATORY

REPORT SIT-DL-72-1589

SEPTEMBER 1972

PROPELLER-RUDDER INTERACTION DUE TO LOADING AND THICKNESS EFFECTS

by

S. Tsakonas
W.R. Jacobs
M.R. Ali

This Research was Sponsored by the Department of Hydromechanics of the Naval Ship Research and Development Center under Contract N00014-67-A-0202-0024

STEVENS INSTITUTE
OF TECHNOLOGY

CASTLE POINT STATION
HOBOKEN, NEW JERSEY 07030

R-1589

64

DAVIDSON LABORATORY

Report SIT-DL-72-1589

September 1972

PROPELLER-RUDDER INTERACTION DUE TO LOADING AND THICKNESS EFFECTS

by

S. Tsakonas, W.R. Jacobs and M.R. Ali

This Research was sponsored by the Naval Ship Research and Development Center, General Hydromechanics Research Program under Contract N00014-67-A-0202-0024 (DL Project 3764/122)

Approved

J.P. Breslin, Director

viii + 42 pp.
11 Figures
1 Appendix (2 pp.)

DOCUMENT CONTROL DATA - R & D

Security classification of title, body of abstract and indexing annotation must be entered when the overall report is classified)

1. ORIGINATING ACTIVITY (Corporate author)
Davidson Laboratory
Stevens Institute of Technology

2a. REPORT SECURITY CLASSIFICATION
Unclassified

2b. GROUP

3. REPORT TITLE

PROPELLER-RUDDER INTERACTION DUE TO LOADING AND THICKNESS EFFECTS

4. DESCRIPTIVE NOTES (Type of report and, inclusive dates)
Final

5. AUTHOR(S) (First name, middle initial, last name)
S. Tsakonas, W.R. Jacobs, M.R. Ali

6. REPORT DATE
September 1972

7a. TOTAL NO. OF PAGES
63

7b. NO. OF REFS
16

8a. CONTRACT OR GRANT NO.
N00014-67-A-0202-0024

b. PROJECT NO.

c.

d.

9a. ORIGINATOR'S REPORT NUMBER(S)
R-1589

9b. OTHER REPORT NO(S) (Any other numbers that may be assigned this report)

10. DISTRIBUTION STATEMENT
Distribution of this document is unlimited.

11. SUPPLEMENTARY NOTES

12. SPONSORING MILITARY ACTIVITY
Department of Hydromechanics
Naval Ship Research and Development Center
Washington, D.C.

13. ABSTRACT

The previous analysis of the propeller-rudder interaction problem by means of the lifting surface theory has been modified to include the effects of thickness of both surfaces.

The effect of thickness on the "flow displacement" in the field is taken into account by the "thin body" approach. The blade thickness effect on the loading of the propeller blade due to its non-planar form, being small, is neglected. The resulting onset velocities on both lifting surfaces due to the thickness effects on the flow field are incorporated, together with the onset velocities due to hull wake and camber and incident angle of the surfaces, into the existing iterative procedure. The numerical procedure, adapted to the CDC-6600 high-speed digital computer, furnishes the steady and time-dependent pressure distributions on both lifting surfaces and the resulting hydrodynamic forces and moments.

From the limited number of calculations, it is seen that the mean and blade-frequency thrust and torque and the mean rudder force and moment are very little affected by the thickness even at the smallest possible axial clearance between propeller and rudder. The influence of thickness is greater on the propeller bearing forces and bending moments, and decreases with increase in axial clearance. The thickness effect is most pronounced in the case of unsteady rudder forces and moments at certain axial clearances, varying cyclically with clearance.

14. KEY WORDS	LINK A		LINK B		LINK C	
	ROLE	WT	ROLE	WT	ROLE	WT
Hydrodynamics Unsteady Theory for Propeller-Rudder Interaction						

TABLE OF CONTENTS

NOMENCLATURE

A_R	area of rudder
a	Ω/U
C	expanded blade chord length
C_R	semichord of rudder
D	propeller diameter
$F(k,m,\rho)$	defined in Equation 21
$F_{x,y,z}$	propeller hydrodynamic forces
F_R	side force on rudder
$f(\xi,\rho,\theta_o)$	thickness distribution on one side of propeller blade section
$f(\xi,\eta,\zeta)$	thickness distribution on one side of rudder section
$I^{(\bar{m})}(f)$	defined in Appendix
$I_m(\ )$	modified Bessel function of order m
$(IK)_m$	defined in Equations 17 and 27
i	index
$J_m(\ )$	Bessel function of order m
j	index
$K_m(\ )$	modified Bessel function of order m
K_{ji}	kernel of integral equation
$\bar{K}_{ji}$	kernel after chordwise integrations
k	variable of integration
k	positive numerical index
L'	loading, lb/ft^2
$L^{(\lambda_k,\bar{n})}$	spanwise loading components, lb/ft (coefficients of Birnbaum distribution)

Nomenclature

ℓ	integer multiple
$M(\ )$	source strength density
M_R	moment about rudder stock
$\bar{m}$	order of lift operator
m	index of summation
N	number of blades
$\bar{n}$	order of chordwise mode
n	blade index
n	r.p.s.
P	subscript index of propeller
$Q_{x,y,z}$	propeller hydrodynamic moments
q	order of blade harmonic
R	subscript index of rudder
R	Descartes distance
r	radial coordinate
r	superscript index of dependence on r
r_o	propeller radius
S	lifting surface
s	coordinate along helicoidal surface
t	time, sec
t_o	maximum thickness of section
t_P	thickness of propeller blade section
t_R	thickness of rudder section

Nomenclature

U	uniform velocity
W_P	onset velocity normal to propeller blade
W_R	onset velocity normal to rudder
W_{R_tP}	onset velocity normal to propeller blade due to rudder thickness
W_{P_tR}	onset velocity normal to rudder due to propeller blade thickness
$\bar{W}_j$	onset velocity after chordwise integration
x	longitudinal ordinate
x, r, φ	cylindrical coordinate system
x, y, z	Cartesian coordinate system of rudder
x_o	distance between propeller plane and rudder stock (see Figure 1)
y	horizontal ordinate on rudder
z	vertical ordinate on rudder
δ	rudder angle
e_R	distance between rudder stock and rudder midchord (see Figure 1)
ζ	vertical ordinate on rudder
η	horizontal ordinate on rudder
θ	angular coordinate
θ_o	angular position of point on propeller blade with respect to midchord line
θ_α	angular chordwise location
θ_b	projected propeller semichord length, radians
θ_n	$\frac{2\pi}{N}(n-1)$, $n = 1,....N$
λ	variable of integration
λ_k	positive integer multiple

Nomenclature

ξ	longitudinal ordinate
ξ, ρ, θ	cylindrical coordinate system
ξ, η, ζ	Cartesian coordinate system of rudder
ρ	radial coordinate
ρ	superscript index of dependence on ρ
ρ_f	mass density of fluid
σ	angular measure of skewness
Φ	velocity potential
$\Phi(\bar{m})$	generalized lift operator (see Appendix)
φ	angular coordinate
φ_o	angular position of point on propeller blade with respect to midchord line
φ_α	angular chordwise location
Ω	angular velocity of propeller

Coefficients

$$K_{F_{x,y,z}} = \frac{F_{x,y,z}}{\rho_f n^2 D^4}$$

$$K_{Q_{x,y,z}} = \frac{Q_{x,y,z}}{\rho_f n^2 D^5}$$

$$C_{F_R} = \frac{F_R}{\frac{\rho_f}{2} A_R U^2}$$

$$C_{M_R} = \frac{M_R}{\frac{\rho_f}{2} A_R U^2 (2C_R)}$$

INTRODUCTION

This study, which includes the effects of thickness of both components of the interacting lifting surfaces, supplements the theoretical investigation[1] conducted at Davidson Laboratory which treated the lifting problem of the propeller-rudder interaction under realistic flow conditions and considering the actual geometry of both lifting surfaces, but neglecting thickness. Reference 1 was an extension of a series of investigations conducted at Davidson Laboratory[2-6] which were concerned with adapting the lifting surface theory to the marine propeller. It developed a numerical solution to provide a calculation procedure adaptable to the CDC6600 high-speed computer for evaluating the steady and time-dependent pressure distributions on both lifting surfaces and the corresponding hydrodynamic forces and moments.

The pair of simultaneous surface integral equations expressing the kinematic boundary conditions on the two interacting lifting surfaces was solved by using the previously developed method of[2-6] evaluating the loading on propeller blades rotating in a known wake, and the method developed in Reference 7 for determining the loading on a finite aspect ratio hydrofoil operating in a known flow field or undergoing prescribed motions. In all of these investigations the lifting problem has been treated by means of the acceleration potential in terms of pressure doublets with axes in the direction of the local normal and strength equal to the pressure jump across the surface.

Although the calculated hydrodynamic forces and moments of Reference 1 agree as far as trends in terms of various parameters are concerned with engineering experience[8,9,10], no quantitative comparison could be made because of the omission of thickness effects. However, before embarking on a study of the thickness effects, a critical review of the analysis and numerical procedure and corresponding program of Reference 1 has been undertaken in the attempt to explain why the results have shown

the calculated vibratory force on the rudder and the rudder-stock moment to be quite high compared with experimental values.

It has been found that the numerical procedure employed in Reference 1 for the cross-coupling kernel terms is not appropriate and could lead to serious problems. Specifically, the cross-coupling term which indicates the influence of the propeller on the rudder and has a high-order singularity combined with a Cauchy-type singularity was inadequately treated.

A new numerical procedure has been developed and the existing program for the propeller-rudder interaction problem has been modified accordingly. A comparison of the hydrodynamic forces and moments calculated by the modified program with earlier results shows a great improvement in the vibratory values of rudder side force and rudder-stock moment.

With this improvement achieved, the analysis of the thickness effects of propeller and rudder could be undertaken. These effects are twofold in origin, 1) due to the fact that the blade surface is nonplanar and 2) due to the "displacement" of the flow caused by the thickness of both lifting surfaces.

When the surfaces are nonplanar, e.g., the helicoidal surfaces of propeller blades, the thickness of the surface will induce a continuous component of velocity on points of the surface itself. In this case thickness effects can be obtained by a distribution of pressure sources with strength equal to the local discontinuity of the normal acceleration.

In a concurrent investigation of the effect of thickness of propeller blades on the propeller loading[11] this effect has been found to be small. In addition, it can only be evaluated accurately when incorporated in the time-consuming numerical procedure derived from the "exact" treatment of the helicoidal wake of the blade.[12] Since the iterative process of the present solution of the interaction problem[1] is already lengthy, the simplified numerical procedure for calculating propeller loading must be used, based on the "staircase" approximation of the helicoidal blade wake. Therefore the small effect on the loading of the nonplanar thickness of the propeller will be neglected here.

The second effect, due to the "flow distortion" caused by the thickness of both lifting surfaces, has an important effect, as has been seen in Reference 13, on the velocity generated by the operating propeller. This contributing factor is taken into account in the present study by means of the "thin body" approximation and has been incorporated in the existing mechanics of the iterative procedure for the solution of the propeller-rudder interaction problem.

This research was sponsored by the Naval Ship Research and Development Center, General Hydromechanics Research Program under Contract N00014-14-67-A-0202-0024 (DL Project 3764/122).

STATEMENT OF THE PROBLEM

A propeller and a rudder of arbitrary geometry are immersed in the wake of a hull. Both surfaces are therefore operating in the nonuniform flow field existing behind the hull and assumed to be that of an ideal incompressible fluid. The propeller-rudder arrangement is shown in Figure 1.

On the basis of the linearized unsteady lifting surface theory, the kinematic boundary conditions on both lifting surfaces are expressed as a pair of surface integral equations:

$$W_P(x_P, r_P, \varphi_P; t) = \int\int_{S_P} L'_P(\xi_P, \rho_P, \theta_P; t)\, K_{PP}(x_P, r_P, \varphi_P; \xi_P, \rho_P, \theta_P; t)\, d\, S_P + \int\int_{S_R} L'_R(\xi_R, 0, \zeta_R; t)\, K_{RP}(x_P, r_P, \varphi_P; \xi_R, 0, \zeta_R; t)\, d\, S_R \quad (1)$$

$$W_R(x_R, 0, z_R; t) = \int\int_{S_P} L'_P(\xi_P, \rho_P, \theta_P; t)\, K_{PR}(x_R, 0, z_R; \xi_P, \rho_P, \theta_P; t)\, d\, S_P + \int\int_{S_R} L'_R(\xi_R, 0, \zeta_R; t)\, K_{RR}(x_R, 0, z_R; \xi_R, 0, \zeta_R)\, d\, S_R \quad (2)$$

where x, r, φ and ξ, ρ, θ: cylindrical coordinates of control and loading points, respectively, associated with the propeller

x, y, z and ξ, η, ζ: Cartesian coordinates of the corresponding points associated with the rudder

t: time, sec.

S_P, S_R: propeller and rudder surfaces, respectively, ft^2

W_P, W_R: onset velocity distributions normal to propeller and rudder, respectively, ft/sec

L'_P, L'_R: unknown loading on propeller blade and rudder, respectively, lb/ft^2

K_{ji}: induced velocity on element i due to oscillatory load of unit amplitude located at element j, ft/lb sec

It is more convenient to use cylindrical coordinates (x, r, φ) and (ξ, ρ, θ) for the rudder also. These are related to the Cartesian coordinates (x, y, z) and (ξ, η, ζ) in the following manner:

$$y_R = \lim_{\varphi_R \to \substack{0 \\ \pi}} (r_R \sin\varphi_R) \qquad \eta_R = \lim_{\theta_R \to \substack{0 \\ \pi}} (\rho_R \sin\theta_R)$$

$$z_R = \lim_{\varphi_R \to \substack{0 \\ \pi}} (r_R \cos\varphi_R) \qquad \zeta_R = \lim_{\theta_R \to \substack{0 \\ \pi}} (\rho_R \cos\theta_R) \tag{3}$$

where φ_R, $\theta_R = 0$ when z_R, $\zeta_R > 0$ and φ_R, $\theta_R = \pi$ when z_R, $\zeta_R < 0$.

The second term on the right-hand side of Equation (1) and the first term on the right-hand side of Equation (2) represent the interference effect of the rudder on the propeller and of the propeller on the rudder, respectively. The remaining terms of Equations (1) and (2) represent the contribution to the flow induced by each surface upon itself.

The oscillatory loading and the prescribed onset velocity can be expressed as

$$L_j'(\xi, \rho, \theta; t) = \text{R.P.} \sum_{\lambda_k = 0}^{\infty} L_j'^{(\lambda_k)}(\xi, \rho, \theta) e^{i\lambda_k \Omega t}$$

$$W_j(x, r, \varphi; t) = \text{R.P.} \sum_{q=0}^{\infty} W_j^{(q)}(x, r, \varphi) e^{iq\Omega t} \tag{4}$$

where Ω is angular velocity of the propeller, and λ_k and q are positive integers. $L^{(\lambda)}$ and $W^{(q)}$ are the complex conjugates of their corresponding values.

The surface integral equations (1) and (2) are reduced to line integral equations by use of the mode approach,[5,7] where $\bar{n}$ terms of the Birnbaum chordwise modes are taken as the unknown chordwise distribution of loading, and by application of the "generalized" lift operator[5,7] of $\bar{m}$ modes to both sides of the equations, thus permitting the chordwise integration to be performed analytically. After the chordwise (θ and φ) integrations, Equations (1) and (2) may be represented for a given frequency q as

$$\sum_{\bar{m}=1}^{\bar{n}} \bar{W}_P^{(q,\bar{m})}(x_p, r_p, \varphi_p) e^{iq\Omega t} =$$

$$\int_{\rho_p} \sum_{\lambda_1=0}^{\infty} \sum_{\bar{m}=1}^{\bar{n}} \sum_{\bar{n}=1}^{\bar{n}} L_p^{(\lambda_1,\bar{n})}(\rho_p) e^{i\lambda_1\Omega t} \bar{K}_{PP}^{(\bar{m},\bar{n})} d\rho_p$$

$$+ \int_{\zeta_R} \sum_{\lambda_2=0}^{\infty} \sum_{\bar{m}=1}^{\bar{n}} \sum_{\bar{n}=1}^{\bar{n}} L_R^{(\lambda_2,\bar{n})}(\zeta_R) e^{i\lambda_2\Omega t} \bar{K}_{RP}^{(\bar{m},\bar{n})} d\zeta_R \qquad (5)$$

$$\sum_{\bar{m}=1}^{\bar{n}} \bar{W}_R^{(q,\bar{m})}(x_R, r_R, \varphi_R) e^{iq\Omega t} =$$

$$\int_{\rho_p} \sum_{\lambda_3=0}^{\infty} \sum_{\bar{m}=1}^{\bar{n}} \sum_{\bar{n}=1}^{\bar{n}} L_p^{(\lambda_3,\bar{n})}(\rho_p) e^{i\lambda_3\Omega t} \bar{K}_{PR}^{(\bar{m},\bar{n})} d\rho_p$$

$$+ \int_{\zeta_R} \sum_{\lambda_4=0} \sum_{\bar{m}=1}^{\bar{n}} \sum_{\bar{n}=1}^{\bar{n}} L_R^{(\lambda_4,\bar{n})}(\zeta_R) e^{i\lambda_4\Omega t} \bar{K}_{RR}^{(\bar{m},\bar{n})} d\zeta_R \qquad (6)$$

where the superscripts $\bar{m}$ and $\bar{n}$ refer to the orders of the lift operator and the assumed chordwise mode, respectively, the bars over W and K indicate that the chordwise integrations (i.e., θ and φ integrations) have been performed, L_j is spanwise loading in lb/ft and λ_k an integer which has been determined in the course of development of the kernels.[1]

Then the set of $\bar{m} = \bar{n}$ line integral equations is solved by the collocation method. In this method, the spans of propeller and rudder are divided into strips of small lengths. The spanwise loading is considered constant over each strip, hence only the kernel need be integrated over the span. With these simplifications, the integral equations (5) and (6) are converted to a system of simultaneous algebraic equations.

Since in the linearized theory the principle of superposition applies, the various flow disturbances (on the left-hand side of the equations) can be treated separately and their effects added. The flow disturbances considered in Reference 1 were those due to hull wake and to incidence angle and camber of propeller blades and rudder. In this study, while the effect of blade thickness on the blade surface itself will be neglected as very small (see Ref. 11), the effect of blade thickness on the velocity field of the rudder and the effect of rudder thickness on the velocity distribution at the propeller is evaluated.

ONSET VELOCITIES DUE TO THICKNESS EFFECTS

Effect of Propeller Blade Thickness

The effect of finite blade thickness is to produce a symmetrical disturbance of the fluid on each side of the surface of symmetry through the blade sections. The basic mathematical model for such symmetrical flows is a combination of sources and sinks. Following the development of the thickness effect on the pressure field presented in Reference 14, the thickness distribution of the blade section is approximated by a source-sink array and the velocity potential for this array is given, in the case of an N-bladed propeller, as

$$\Phi(x,r,\varphi;t) = \frac{1}{4\pi} \sum_{n=1}^{N} \iint_{S} \frac{M(\xi,\rho,\theta_o)}{R}\, dS \qquad (7)$$

where S = surface of the blade

x, r, φ = cylindrical coordinates of a field point

ξ, ρ, θ = cylindrical coordinates of a point on the propeller blade

$M(\xi,\rho,\theta_o) = 2U \dfrac{\partial f(\xi,\rho,\theta_o)}{\partial \xi}$, source strength density

$= 2U\sqrt{1+a^2\rho^2}\, \dfrac{\partial f(\rho,s)}{\partial s}$ where s is coodinate along the helicoidal surface and $a = \Omega/U$

U = free stream velocity

$\dfrac{\partial f(\xi,\rho,\theta_o)}{\partial \xi}$ = slope of blade section

$R = \left\{(x-\xi)^2 + r^2 + \rho^2 - 2r\rho\cos(\theta-\varphi+\bar{\theta}_n)\right\}^{\frac{1}{2}}$

$\bar{\theta}_n = \dfrac{2\pi}{N}(n-1)$

$\theta = \theta_o - \Omega t$

θ_o = angular position of point on propeller blade with respect to the midchord line, i.e., angular position with respect to a system fixed in the propeller

and in the present case the field points x,r,φ are on the rudder.

x,r,φ, the cylindrical coordinates of the rudder, are related to the Cartesian coordinates x,y,z by Equation (3) so that

$$r = |z|$$

$$\varphi = \begin{cases} 0 \text{ when } z > 0 \\ \pi \text{ when } z < 0 \end{cases} \tag{8}$$

From Figure 1 it is seen that

$$x = x_o + e_R - C_R(z)\cos\varphi_\alpha,\ 0 \le \varphi_\alpha \le \pi \tag{9}$$

where φ_α is angular chordwise location of a point on the rudder.

Changing the surface integration over the propeller blade (Equation 7) to that over its projection in the propeller plane yields

$$\Phi(x,r,\varphi;t) = \frac{1}{4\pi} \sum_{n=1}^{N} \int_{-\theta_b^\rho}^{\theta_b^\rho} \int_{\rho} \frac{M(\xi,\rho,\theta_o)}{R} \frac{\sqrt{1+a^2\rho^2}}{a\rho}\, \rho d\rho d\theta_o \tag{10}$$

where θ_b^ρ is projected semichord length of the blade at radius ρ in radians.

With the trigonometric transformation

$$\theta_o = \sigma^\rho - \theta_b^\rho \cos\theta_\alpha,\ 0 \le \theta_\alpha \le \pi \tag{11}$$

where θ_α is angular chordwise location of a point on the projected blade and σ^ρ is angular position of the midchord line from the generator line through the hub, or skewness, at radius ρ, then

$$d\theta_o = \theta_b^\rho \sin\theta_\alpha\, d\theta_\alpha \tag{12}$$

Furthermore, since the helicoidal surface of the blade is given by $\xi = \theta_o/a$

$$\frac{\partial f(\xi, \rho, \theta_o)}{\partial \xi} = \frac{a}{\theta_b^\rho \sin\theta_\alpha} \frac{\partial f(\rho, \theta_\alpha)}{\partial \theta_\alpha} \tag{13}$$

The velocity potential can therefore be written as

$$\Phi(x, r, \varphi; t) = \frac{U}{2\pi} \sum_{n=1}^{N} \int_0^\pi \int_\rho \frac{\partial f(\rho, \theta_\alpha)}{\partial \theta_\alpha} \frac{\sqrt{1+a^2\rho^2}}{R} d\rho d\theta_\alpha \tag{14}$$

Following Reference 15 the thickness distribution is approximated by an ogive section

$$f(\rho, \theta_\alpha) \approx \frac{1}{2} t_o(\rho) \sin^2\theta_\alpha$$

where $t_o(\rho)$ is maximum thickness at radius ρ, or if the ratio of maximum thickness to expanded chord length, $t_o(\rho)/C(\rho)$, is given

$$f(\rho, \theta_\alpha) \approx \frac{t_o(\rho)}{C(\rho)} \rho\theta_b^\rho \frac{\sqrt{1+a^2\rho^2}}{a\rho} \sin^2\theta_\alpha \tag{15}$$

Then

$$\frac{\partial f(\rho, \theta_\alpha)}{\partial \theta_\alpha} \approx \frac{2\sqrt{1+a^2\rho^2}}{a} \theta_b^\rho \frac{t_o(\rho)}{C(\rho)} \sin\theta_\alpha \cos\theta_\alpha \tag{16}$$

On making use of an expansion scheme for the reciprocal of the Descartes distance R, viz.

$$\frac{1}{R} = \frac{1}{\pi} \sum_{m=-\infty}^{\infty} e^{im(\theta_o - \Omega t - \varphi + \tilde{\theta}_n)} \int_{-\infty}^{\infty} (IK)_m e^{i(x-\xi)k} dk \tag{17}$$

where $(IK)_m =$

$$\begin{cases} I_m(|k|\rho) K_m(|k|r) & \text{for } \rho < r \\ I_m(|k|r) K_m(|k|\rho) & \text{for } \rho > r \end{cases}$$

($I_m(\ )$ and $K_m(\ )$ being modified Bessel functions) and by substitution of (16) and the formulas for θ_o and ξ the velocity potential becomes

$$\phi(x,r,\varphi;t) = \frac{U}{\pi^2} \sum_{n=1}^{N} \sum_{m=-\infty}^{\infty} e^{im(\bar{\theta}_n - \Omega t - \varphi)}$$

$$\cdot \int_0^{\pi} \int_{\rho} \left(\frac{1+a^2\rho^2}{a}\right) \frac{t_o(\rho)}{C(\rho)} \theta_b^{\rho} \cos\theta_\alpha \sin\theta_\alpha \int_{-\infty}^{\infty} (IK)_m e^{Ixk} e^{-I(k-am)\frac{\sigma^{\rho}}{a}} e^{I\frac{(k-am)}{a}\theta_b^{\rho}\cos\theta_\alpha}$$

$$dk\,d\rho\,d\theta_\alpha \qquad (18)$$

The integration over θ_α involves

$$I_{\theta_\alpha} = \int_0^{\pi} \cos\theta_\alpha \sin\theta_\alpha\, e^{\frac{I(k-am)}{a}\theta_b^{\rho}\cos\theta_\alpha}\, d\theta_\alpha$$

which is identically zero for $k = am$. In addition, certainly for $k \neq am$,

$$I_{\theta_\alpha} = -I\frac{a\partial}{\theta_b^{\rho}\,\partial(k-am)} \int_0^{\pi} \sin\theta_\alpha e^{I(k-am)\frac{\theta_b^{\rho}}{a}\cos\theta_\alpha}\, d\theta_\alpha$$

$$= \frac{12a^2}{[\theta_b^{\rho}(k-am)]^2} \left\{\sin\left[\frac{(k-am)}{a}\theta_b^{\rho}\right] - \frac{(k-am)}{a}\theta_b^{\rho}\cos\left[\frac{(k-am)}{a}\theta_b^{\rho}\right]\right\} \qquad (19)$$

It can be shown that this too goes to zero when $k = am$. Furthermore,

$$\sum_{n=1}^{N} e^{im\bar{\theta}_n} = \begin{cases} N \text{ for } m = \ell N, \ \ell = 0, \pm 1, \pm 2 \ldots \\ 0 \text{ for } m \neq \ell N \end{cases} \qquad (20)$$

Therefore

$$\phi(x,r,\varphi;t) = \frac{12aNU}{\pi^2} \sum_{\substack{m=-\infty \\ m=\ell N}}^{\infty} e^{-im(\varphi+\Omega t)}$$

$$\cdot \int_{\rho} \frac{t_o(\rho)}{C(\rho)} \frac{(1+a^2\rho^2)}{\theta_b^{\rho}} e^{im\delta} \int_{-\infty}^{\infty} (IK)_m e^{Ik(x-\frac{\rho}{a})} F(k,m,\rho)\,dk\,d\rho \qquad (21)$$

where $F(k,m,\rho) = \dfrac{\left\{\sin\left[\left(\frac{k-am}{a}\right)\theta_b^\rho\right] - \left(\frac{k-am}{a}\right)\theta_b^\rho \cos\left[\left(\frac{k-am}{a}\right)\theta_b^\rho\right]\right\}}{(k-am)^2}$

The velocity normal to the rudder W_{P_tR} due to blade thickness is given by

$$W_{P_tR}(x,r,\varphi;t) = \pm\frac{1}{r}\frac{\partial}{\partial\varphi}\Big|_{\substack{\varphi=0\\ \pi}} \Phi(x,r,\varphi;t)$$

where the positive sign is taken when $\varphi = 0$ and the negative when $\varphi = \pi$. Therefore,

$$W_{P_tR} = \frac{2aNU}{\pi^2 r} \sum_{\substack{m=-\infty\\ m=\ell N}}^{\infty} m \left\{\begin{matrix}+1 \text{ for } z>0\\ -(-1)^m \text{ for } z<0\end{matrix}\right\} e^{-im\Omega t}$$

$$\cdot \int_\rho \frac{t_o(\rho)}{C(\rho)} \frac{(1+a^2\rho^2)}{\theta_b^\rho} e^{im\sigma^\rho} \int_{-\infty}^{\infty} (IK)_m \, e^{ik\left(x-\frac{\sigma^\rho}{a}\right)} F(k,m,\rho)\,dk\,d\rho \quad (22)$$

After substituting the value of x given in Equation (9), the generalized lift operators are applied to Equation (22) on the left hand side as to the right hand side of Equation (2). This is required by the method used in solving the pair of integral equations (see Reference 1).

Thus for each lift operator mode $\bar{m}$ (see the Appendix)

$$\bar{W}_{P_tR}^{(\bar{m})} = \frac{1}{\pi}\int_0^\pi \Phi(\bar{m}) W_{P_tR}\, d\varphi_\alpha$$

This involves the chordwise integral

$$\frac{1}{\pi}\int_0^\pi \Phi(\bar{m}) e^{ik(x_o+\epsilon_R - C_R\cos\varphi_\alpha)}\, d\varphi_\alpha$$

$$= e^{ik(x_o+\epsilon_R)}\, I^{(\bar{m})}(-kC_R)$$

with $I^{(\bar{m})}(f)$ as defined in the Appendix.

After the application of the lift operators Equation (22) becomes for each $\bar{m}$

$$\bar{w}_{P_t R}^{(\bar{m})} = \frac{2aNU}{\pi^2 r} \sum_{\substack{m=-\infty \\ m=\ell N}}^{\infty} m \begin{Bmatrix} +1 \text{ for } z > 0 \\ -(-1)^m \text{ for } z < 0 \end{Bmatrix} e^{-im\Omega t}$$

$$\cdot \int_{\rho} \frac{t_o(\rho)}{C_o(\rho)} \frac{(1+a^2\rho^2)}{\theta_b^{\rho}} e^{im\sigma^{\rho}} \int_{-\infty}^{\infty} (IK)_m e^{ik\left(x_o + e_R - \frac{\sigma^{\rho}}{a}\right)} I^{(\bar{m})}(-kC_R)$$

$$\cdot F(k,m,\rho)dkd\rho \qquad (23)$$

This velocity is 0 when $m = \ell N = 0$, i.e., $\ell = 0$, therefore the propeller thickness does not affect the steady-state rudder loading. For the blade-frequency rudder loading ($\ell = 1$) the time dependence of the L.H. side of the rudder integral equation[1] is represented by exp ($iN\Omega t$). Thus in this case,

$$\bar{w}_{P_t R}^{(\bar{m})} = \left[\bar{w}_{P_t R}^{(-N,\bar{m})} + \text{conj } \bar{w}_{P_t R}^{(N,\bar{m})}\right] e^{iN\Omega t}$$

Then at blade frequency at which $m = N$ the normal velocity on the rudder due to propeller thickness becomes

$$\bar{w}_{P_t R}^{(-N,\bar{m})} + \text{conj } \bar{w}_{P_t R}^{(N,\bar{m})} = \frac{2aN^2U}{\pi^2 r} \begin{Bmatrix} -1 \text{ for } z > 0 \\ (-1)^N \text{ for } z < 0 \end{Bmatrix}$$

$$\cdot \int_{\rho} \frac{t_o(\rho)}{C(\rho)} \frac{(1+a^2\rho^2)}{\theta_b^{\rho}} e^{-iN\sigma^{\rho}} \int_{-\infty}^{\infty} (IK)_N \Big\{ e^{ik\left(x_o + e_R - \frac{\sigma^{\rho}}{a}\right)} I^{(\bar{m})}(-kC_R)$$

$$\cdot F(k,-N,\rho) - e^{-ik\left(x_o + e_R - \frac{\sigma^{\rho}}{a}\right)} I^{(\bar{m})}(kC_R) F(k,N,\rho) \Big\} dkd\rho$$

(24)

If in $F(k,-N,\rho)$, λ is substituted for $k+aN$, and in $F(k,N,\rho)$ λ is substituted for $k-aN$, it can be shown that Equation (24) can be written as

$$\bar{w}_{P_t R}^{(-N,\bar{m})} + \text{conj}\ \bar{w}_{P_t R}^{(N,\bar{m})} = \frac{4aN^2U}{\pi^2 r_R} e^{-iaN(x_o+\epsilon_R)} \begin{cases} 1 \text{ for } z_R > 0 \\ (-1)^N \text{ for } z_R < 0 \end{cases}$$

$$\cdot \int_{\rho_p} \frac{t_o(\rho)}{C(\rho)} \frac{(1+a^2\rho_p^2)}{\theta_b^\rho} \int_o^\infty \frac{\left[\sin \frac{\lambda}{a}\theta_b^\rho - \frac{\lambda}{a}\theta_b^\rho \cos \frac{\lambda}{a}\theta_b^\rho\right]}{\lambda^2}$$

$$\cdot \left\{ I_N(i\lambda - aNi\rho_p) K_N(i\lambda - aNir_R) e^{i\lambda(x_o+\epsilon_R-\frac{\sigma^\rho}{a})} I_1(\bar{m})((aN-\lambda)C_R) \right.$$

$$\left. - I_N(i\lambda + aNi\rho_p) K_N(i\lambda + aNir_R) e^{-i\lambda(x_o+\epsilon_R-\frac{\sigma^\rho}{a})} I_1(\bar{m})((aN+\lambda)C_R) \right\} d\lambda d\rho_p \qquad (25)$$

for $\rho_p < r_R$, otherwise ρ_p and r_R are interchanged in the modified Bessel functions. The subscripts refer to propeller P and rudder R. It can be easily proved that when $\lambda = 0$ the integrand is zero (see earlier Equation 19).

Effect of Rudder Thickness

As in the case of propeller thickness, the effect of the rudder thickness on the flow field will be simulated by a source-sink distribution. Thus the velocity potential due to rudder thickness is given by

$$\Phi(x,r,\varphi;t) = \frac{1}{4\pi} \int_\zeta \int_\xi \frac{M(\xi,\eta,\zeta)}{R} d\xi d\zeta \qquad (26)$$

where $M(\xi,\eta,\zeta) = 2U \frac{\partial f(\xi,\eta,\zeta)}{\partial \xi}$, source strength density

$f(\xi,\eta,\zeta)$ = thickness distribution on one side of the axisymmetric rudder

$R = \left\{(x-\xi)^2 + (r\sin\varphi-\eta)^2 + (r\cos\varphi-\zeta)^2\right\}^{\frac{1}{2}}$

x, r, φ = cylindrical coordinates of a point on the propeller blade

ξ, η, ζ = Cartesian coordinates of a point on the rudder

$\varphi = \varphi_o - \Omega t$

φ_o = angular position of point on propeller with respect to midchord line (in moving coordinate system)

$\xi = x_o + e_R - C_R(\zeta)\cos\theta_\alpha$ (see Figure 1)

θ_α = angular chordwise location of point on rudder

$d\xi = C_R(\zeta)\sin\theta_\alpha\, d\theta_\alpha$

If cylindrical coordinates ξ, ρ, θ are used for the rudder (see Equation 3)

$$\rho = |\zeta|$$

$$\theta = \begin{cases} 0 \text{ when } \zeta > 0 \\ \pi \text{ when } \zeta < 0 \end{cases}$$

$$R = \left\{(x-\xi)^2 + r^2 + \rho^2 - 2r\rho\cos(\theta - \varphi_o + \Omega t)\right\}^{\frac{1}{2}}$$

By means of an expansion scheme the reciprocal of the Descartes distance R can be expressed as

$$\frac{1}{R} = \frac{1}{\pi}\sum_{m=-\infty}^{\infty} e^{im(\theta-\varphi_o+\Omega t)} \int_{-\infty}^{\infty} (IK)_m\, e^{i(x-\xi)k}\, dk \qquad (27)$$

where $(IK)_m = \begin{cases} I_m(|k|\rho)K_m(|k|r) \text{ for } \rho < r \\ I_m(|k|r)K_m(|k|\rho) \text{ for } \rho > r \end{cases}$

It is to be noted that, in contrast to the preceding section, x, r, φ and φ_α are referred to the propeller and ξ, ρ, θ and θ_α to the rudder. Subscripts as shown in Equations (1), (2), (5) and (6) are omitted for convenience in writing.

The thickness distribution can be represented accurately enough by

$$f(\xi, \eta, \zeta) \approx \frac{t_o(\zeta)}{2}\sin^2\theta_\alpha \qquad (28)$$

where $t_o(\zeta)$ is maximum thickness at each section at various ζ. The slope of the rudder section is then

$$\frac{\partial f(\xi,\eta,\zeta)}{\partial \xi} = \frac{1}{C_R(\zeta)\sin\theta_\alpha}\frac{\partial f(\theta_\alpha,\zeta)}{\partial \theta_\alpha} \approx \frac{t_o(\zeta)}{C_R(\zeta)}\cos\theta_\alpha \tag{29}$$

With Equations (27) - (29) the velocity potential becomes

$$\Phi(x,r,\varphi;t) = \frac{U}{2\pi^2}\sum_{m=-\infty}^{\infty} e^{im(\theta-\varphi_o+\Omega t)}$$

$$\cdot \int_o^{\pi}\int_{\zeta} t_o(\zeta)\cos\theta_\alpha \sin\theta_\alpha \int_{-\infty}^{\infty} (IK)_m e^{i(x-x_o-\epsilon_R)k} e^{iC_R(\zeta)\cos\theta_\alpha k}\, dk d\zeta d\theta_\alpha \tag{30}$$

where $\theta = 0$ or π as previously indicated.

The normal velocity to the propeller blade W_{R_tP} due to rudder thickness (a new contributing factor on the left-hand side of Equation (1)) is obtained by taking the derivative of the velocity potential with respect to the normal to the helicoidal blade surface which is given by $x = \varphi_o/a$. At any point (x,r,φ) on the propeller blade this normal derivative is

$$\frac{\partial}{\partial n'} = \frac{r}{\sqrt{1+a^2r^2}}\left(a\frac{\partial}{\partial x} - \frac{1}{r^2}\frac{\partial}{\partial \varphi_o}\right)$$

Then

$$W_{R_tP}(x,r,\varphi;t) = \lim_{x\to\varphi_o/a} \frac{\partial}{\partial n'}\Phi(x,r,\varphi;t)$$

$$= \lim_{x\to\varphi_o/a} \frac{iU}{2\pi^2}\frac{r}{\sqrt{1+a^2r^2}}\sum_{m=-\infty}^{\infty} e^{im(\theta-\varphi_o+\Omega t)}\int_o^{\pi}\int_{\zeta} t_o(\zeta)\cos\theta_\alpha\sin\theta_\alpha$$

$$\cdot \int_{-\infty}^{\infty}\left(ak+\frac{m}{r^2}\right)(IK)_m e^{i(x-x_o-\epsilon_R)k} e^{ikC_R(\zeta)\cos\theta_\alpha}\, dk d\zeta d\theta_\alpha \tag{31}$$

where $\theta = 0$ or π.

The integration over θ_α yields

$$\int_0^\pi \cos\theta_\alpha \sin\theta_\alpha e^{ikC_R(\zeta)\cos\theta_\alpha} d\theta_\alpha = \frac{-i}{C_R(\zeta)} \frac{\partial}{\partial k} \int_0^\pi \sin\theta_\alpha e^{ikC_R(\zeta)\cos\theta_\alpha} d\theta_\alpha$$

$$= \frac{2i}{(kC_R)^2} [\sin(kC_R) - kC_R\cos(kC_R)] \qquad (32)$$

which is zero when $k = 0$ (see Equation 19). Equation (32) is substituted in (31) and the limit $x \to \varphi_o/a$ is taken. Since the integer m can only take the values of q (the harmonics of the propeller blade loading, $q \geq 0$) i.e.,

$$W_{R_t P}(x, r, \varphi; t) = W_{R_t P}^{(q)} e^{iq\Omega t} \qquad (33)$$

(see Equation 4 and Reference 1), the normal velocity component $W_{R_t P}^{(q)}$ becomes

$$W_{R_t P}^{(q)} = -\frac{U}{\pi^2} \frac{r}{\sqrt{1+a^2r^2}} \int_\zeta \begin{Bmatrix} (-1)^q & \text{for } \zeta < 0 \\ +1 & \text{for } \zeta > 0 \end{Bmatrix} \cdot \frac{t_o(\zeta)}{C_R(\zeta)}$$

$$\cdot \int_{-\infty}^{\infty} \left(a + \frac{q}{r^2 k}\right) \left[\frac{\sin kC_R(\zeta)}{kC_R(\zeta)} - \cos kC_R(\zeta)\right] (IK)_q$$

$$\cdot e^{-i(x_o + e_R)k} e^{i\left(\frac{k}{a} - q\right)\varphi_o} dk d\zeta \qquad (34)$$

With the transformation

$$\varphi_o = \sigma^r - \theta_b^r \cos\varphi_\alpha \qquad (35)$$

where φ_α is angular chordwise location of a point on the blade, θ_b^r is projected semichord length of the propeller blade at radius r in radians, and σ^r is angular position of the midchord line from the generator line through the hub, or skewness, at that radius, the generalized lift operators can be applied to $W_{R_t P}$ as to the RH of the integral equation (1) (see Reference 1). Thus for each lift operator mode $\bar{m}$

$$\bar{W}_{R_t P}^{(q,\bar{m})} = \frac{1}{\pi}\int_0^{\pi} \epsilon(\bar{m}) W_{R_t P}^{(q)}\, d\varphi_\alpha \tag{36}$$

The φ_α-integration involves

$$\frac{1}{\pi}\int_0^{\pi} \epsilon(\bar{m}) e^{i(\frac{k}{a}-q)\varphi_o}\, d\varphi_\alpha = e^{i(\frac{k}{a}-q)\sigma^r}\left\{\frac{1}{\pi}\int_0^{\pi} \epsilon(\bar{m}) e^{i(q-\frac{k}{a})\theta_b^r \cos\varphi_\alpha}\, d\varphi_\alpha\right\}$$

$$= e^{i(\frac{k}{a}-q)\sigma^r} I^{(\bar{m})}((q-\tfrac{k}{a})\theta_b^r) \tag{37}$$

where $I^{(\bar{m})}(f)$ is defined in the Appendix.

Therefore Equation (36) can be written as

$$\bar{W}_{R_t P}^{(q,\bar{m})} = -\frac{U}{\pi^2}\frac{r_P e^{-iq\sigma^r}}{\sqrt{1+a^2 r_P^2}}\int_{\zeta_R}\left\{\begin{matrix}(-1)^q \text{ for } \zeta_R<0\\ +1 \quad \text{for } \zeta_R>0\end{matrix}\right\}\frac{t_o(\zeta)}{C_R(\zeta)}\int_0^{\infty}(IK)_q\left[\frac{\sin kC_R(\zeta)}{kC_R(\zeta)} - \cos kC_R(\zeta)\right]$$

$$\cdot\left\{(a+\frac{q}{r_P^2 k})e^{-i(x_o+\epsilon_R-\frac{\sigma^r}{a})k} I^{(\bar{m})}((q-\tfrac{k}{a})\theta_b^r)\right.$$

$$\left.+(a-\frac{q}{r_P^2 k})e^{i(x_o+\epsilon_R-\frac{\sigma^r}{a})k} I^{(\bar{m})}((q+\tfrac{k}{a})\theta_b^r)\right\} dk\, d\zeta_R \tag{38}$$

where the range of integration has been converted to positive k. When $k = 0$ the integrand is zero for all q (see Equation 32).

NUMERICAL RESULTS

The normal velocity distribution on either of two interacting surfaces due to the flow disturbance caused by the thickness of the other has been evaluated in the case of a propeller-rudder configuration by means of the "thin body" approximation. These normal velocities caused by flow disturbances other than hull wake, camber and incidence angle which were treated in Reference 1 will be added to the others to form a new set of onset velocity distributions on the interacting surfaces.

Thus Equation 38 representing the velocity normal to the propeller blades due to rudder thickness t_R is added, at the appropriate frequency q, to the normal velocity $\bar{W}_P^{(q,\bar{m})}$ (left-hand side of Equation 5) attributed to all other flow disturbances mentioned above. Equation 25 representing the normal velocity to the rudder due to propeller blade thickness t_p should be added to $\bar{W}_R^{(q,\bar{m})}$ (left-hand side of Equation 6) at blade frequency q = N. In the latter case, in fact, the propeller thickness effect will be the only contributor to $\bar{W}_R^{(q,\bar{m})}$. There is no contribution from blade thickness to $\bar{W}_R^{(o,\bar{m})}$ the steady-state normal velocity which is due to rudder angle of attack and rudder camber if any.

With the addition of these thickness effects, the iteration procedure developed in Reference 1 for the numerical solution of the propeller-rudder interaction problem is employed again. The solution evaluates the steady and time-dependent pressure distributions on both lifting surfaces and the resulting hydrodynamic forces F_x, F_y and F_z and moments Q_x, Q_y and Q_z on the propeller and the rudder side force F_R and rudder-stock moment M_R.

The iterative procedure is illustrated below for an N-blade propeller and q = 0 to N+1 (cf Reference 1).

0-iteration

$$q = 0 \quad , \quad L_{P0}^{(o,\bar{n})} = \left\{ \bar{W}_P^{(o,\bar{m})} + \bar{W}_{R_t P}^{(o,\bar{m})} \right\} \left[\bar{K}_{PP}^{(\bar{m},\bar{n})}(q = 0) \right]^{-1}$$

$$q = N+1, \quad L_{P0}^{(N+1,\bar{n})} = \left\{ \bar{W}_P^{(N+1,\bar{m})} + \bar{W}_{R_t P}^{(N+1,\bar{m})} \right\} \left[\bar{K}_{PP}^{(\bar{m},\bar{n})}(q=N+1) \right]^{-1}$$

$$q = 0 \quad , \quad L_{R1}^{(o,\bar{n})} = \left\{ \bar{U}\delta - L_{P0}^{(o,\bar{n})} \bar{K}_{PR}^{(o,\bar{m},\bar{n})} - L_{P0}^{(1,\bar{n})} \bar{K}_{PR}^{(1,\bar{m},\bar{n})} - L_{P0}^{(2,\bar{n})} \bar{K}_{PR}^{(2,\bar{m},\bar{n})} \right.$$

$$\left. \text{---- } - L_{P0}^{(N+1,\bar{n})} \bar{K}_{PR}^{(N+1,\bar{n})} \right\} \left[\bar{K}_{RR}(q=0) \right]^{-1}$$

$$q = N \quad , \quad L_{R1}^{(N,\bar{n})} = \left\{ \left[\bar{W}_{P_t R}^{(-N,\bar{m})} + \text{conj.} \bar{W}_{P_t R}^{(N,\bar{m})} \right] - \left[L_{P0}^{(o,\bar{n})} \bar{K}_{PR}^{(-N,\bar{m},\bar{n})} \right.\right.$$

$$\left.\left. + L_{P0}^{(1,\bar{n})} \bar{K}_{PR}^{(-N+1,\bar{m},\bar{n})} + L_{P0}^{(2,\bar{n})} \bar{K}_{PR}^{(-N+2,\bar{m},\bar{n})} + \cdots \right] \right\} \left[\bar{K}_{RR}(q=N) \right]^{-1}$$

$$- \text{conj.} \left\{ L_{P0}^{(o,\bar{n})} \bar{K}_{PR}^{(N,\bar{m},\bar{n})} + L_{P0}^{(1,\bar{n})} \bar{K}_{PR}^{(N+1,\bar{m},\bar{n})} + \cdots \right\} \left[\bar{K}_{RR}(q=N) \right]^{-1}$$

where δ = rudder angle and $\bar{U}\delta = U\delta 1^{(\bar{m})}(o)$ is the velocity component due to rudder angle after the lift operators have been applied.

1-iteration

$$q = 0 \quad , \quad L_{P1}^{(o,\bar{n})} = \left\{ \bar{W}_P^{(o,m)} + \bar{W}_{R_t P}^{(o,\bar{m})} - L_{R1}^{(o,\bar{n})} K_{RP}^{(o,\bar{m},\bar{n})} - L_{R1}^{(N,\bar{n})} \bar{K}_{RP}^{(-N,\bar{m},\bar{n})} \right\} \left[\bar{K}_{PP}^{(\bar{m},\bar{n})}(q=o) \right]^{-1}$$

$$q = N+1, \quad L_{P1}^{(N+1,\bar{n})} = \left\{ \bar{W}_P^{(N+1,\bar{m})} + \bar{W}_{R_t P}^{(N+1,\bar{m})} - L_{R1}^{(o,\bar{n})} K_{RP}^{(N+1,\bar{m},\bar{n})} - L_{R1}^{(N,n)} \bar{R}_{RP}^{(1,\bar{m},\bar{n})} \right\}$$

$$\cdot \left[\bar{R}_{PP}^{(\bar{m},\bar{n})}(q=N+1) \right]^{-1}$$

$$q = 0\ ,\ L_{R2}^{(o,\bar{n})} = \left\{ U\delta - L_{P1}^{(o,\bar{n})} \bar{K}_{PR}^{(o,\bar{m},\bar{n})} - L_{P1}^{(1,\bar{n})} \bar{K}_{PR}^{(1,\bar{m},\bar{n})} - \ldots - L_{P1}^{(N+1,\bar{n})} \bar{K}_{PR}^{(N+1,\bar{m},\bar{n})} \right\} \left[\bar{K}_{RR}^{(q=o)} \right]^{-1}$$

$$q = N\ ,\ L_{R2}^{(N,\bar{n})} = \left\{ \left[\bar{W}_{P_t R}^{(-N,\bar{m})} + \text{conj.} \bar{W}_{P_t R}^{(N,\bar{m})} \right] - \left[L_{P1}^{(o,\bar{n})} \bar{K}_{PR}^{(-N,\bar{m},\bar{n})} + L_{P1}^{(1,\bar{n})} \bar{K}_{PR}^{(-N+1,\bar{m},\bar{n})} \right.\right.$$

$$\left.\left. + \ldots + L_{P1}^{(N+1,\bar{n})} \bar{K}_{PR}^{(1,\bar{m},\bar{n})} \right] \right\} \left[\bar{K}_{RR}^{(q=N)} \right]^{-1}$$

$$- \text{conj.} \left\{ L_{P1}^{(o,\bar{n})} \bar{K}_{PR}^{(N,\bar{m},\bar{n})} + L_{P1}^{(1,\bar{n})} \bar{K}_{PR}^{(N+1,\bar{m},\bar{n})} + \ldots \right\} \left[\bar{K}_{RR}^{(q=N)} \right]^{-1}$$

Usually four iterations are sufficient to achieve stabilized values of the loadings on propeller and rudder, L_P and L_R, respectively.

Before incorporating the thickness effects into the existing program as shown above, a new, more precise numerical procedure was introduced for the evaluation of the finite contribution of the high-order singularity in the cross-coupling kernel term K_{PR} which represents the interference effect of the propeller on the rudder.

The modified program has been applied to the case of the hull-propeller-rudder configuration treated in Reference 1. This is the Mod V hull with its designed 4-blade propeller, and rudder of aspect ratio 1.72. The calculations have been performed for three values of axial clearance x_o, the designed clearance to the smallest possible clearance, and for the range of rudder angles from $\delta = +.3$ radian to port to $\delta = -.3$ radian to starboard. It is to be noted that the theoretical development assumes that the ship is steering a straight course or is in the initial stage of turning.

The particulars of the propeller and rudder follow:

Propeller (NSRDC No. 3376)

No. of blades, N	4
Radius, r_o	11 ft
EAR	0.499
P/D	1.10
Advance ratio, J	0.726
Ship Speed, U	28.29 ft/sec

Rudder (see Figure 1)

Semichord, C_R	0.682 r_o
b_u	1.318 r_o
b_c	1.023 r_o
c_R	0.273 r_o
x_o	0.8356 r_o (design)
	0.72 r_o
	0.56 r_o

Tables 1 and 2 compare results of the new modified program with those of Reference 1. It is seen that for steady-state and unsteady flow conditions the differences in the propeller bearing forces and moments are small to moderate. The differences in the steady-state rudder forces and moments are also slight. The greatest change occurs in the vibratory rudder forces and moments. These values are now of the order of magnitude of expected values.

Observations made and conclusions drawn in Reference 1 are still valid. It seems that the present modification has some beneficial influence also on the number of iterations required to obtain stabilized values. The number has been reduced from six to four in all cases under consideration.

Figure 2 graphically exhibits the great change in blade-frequency rudder lateral force and rudder stock moment for a range of rudder angle from $\delta = -0.3$ radians (to starboard) to $\delta = 0.3$ radians (to port), and

Figures 3 and 4 demonstrate the changes in the spanwise distributions of blade-frequency $\tilde{C}_{F_R}$ and $\tilde{C}_{M_R}$ at $\delta = -0.3$, all for the design axial clearance between propeller and rudder, $x_o = 0.8356\ r_o$.

A series of calculations has been performed using this modified program and including the effects of thickness of propeller and rudder, for the same hull-propeller-rudder arrangement. The results for all hydrodynamic forces and moments, with and without thickness effects, are presented in Tables 3(a,b,c), for design clearance $x_o = 0.8356\ r_o$, 4(a,b,c), for $x_o = 0.72\ r_o$, and 5(a,b,c), for $x_o = 0.56\ r_o$ the smallest possible clearance, for a series of rudder angles $\delta = 0, \pm.1, \pm.2, \pm.3$ radians. Graphical presentation of these results, however, has been restricted to the design configuration (Figures 5-9). In addition, Figures 10 and 11 present the spanwise distributions of the blade-frequency rudder side force and rudder stock moment at $\delta = -.3$ for this configuration.

From the limited number of calculations performed, it can be said that the thickness effects do not change the general picture of the interaction problem. This is mainly governed by the trends established before inclusion of thickness. In fact, the change in mean thrust and torque varies from a mere 0.8% for design clearance to 1.1% for the smallest clearance, while the changes in the corresponding vibratory values range from 2 to 5%.

The effect of thickness on the propeller bearing forces and bending moments appears to be almost independent of rudder angle but diminishes monotonically with increase in axial clearance. The curves of these forces and moments are displaced by the following average amounts (to be read with reference to Tables 3, 4 and 5, a, b, in estimating rates of change).

Coefficient	Axial Clearance, x_o		
Mean	0.8356 r_o	0.72 r_o	0.56 r_o
$\Delta\bar{K}_{F_y}$	.00096	.00134	.00240
$\Delta\bar{K}_{Q_y}$	.00057	.00078	.00136
$\Delta\bar{K}_{F_z}$	.00042	.00065	.00091
$\Delta\bar{K}_{Q_z}$	.00017	.00027	.00039
Blade-Frequency			
$\Delta\tilde{K}_{F_y}$	.00002	.00028	.00057
$\Delta\tilde{K}_{Q_y}$	.00010	.00020	.00036
$\Delta\tilde{K}_{F_z}$	.00011	.00016	.00028
$\Delta\tilde{K}_{Q_z}$	.00007	.00010	.00011

Hardly any difference is observed in the values of steady-state rudder side force and rudder-stock moment (see Tables 3c, 4c and 5c). The thickness effects are responsible for only a slight change in the slopes of the steady-state curves versus rudder angle. In the case of the unsteady rudder forces and moments the thickness effect varies cyclically with axial clearance x_o. The effect is negligible for x_o = 0.72 of propeller radius, largest at x_o = 0.56 r_o (at zero rudder angle there is a change in rudder side force of 88% and in rudder-stock moment of 24%), and not so large but significant at x_o = 0.8356 r_o (the corresponding changes are 43% and 7%). The periodic variation of the vibratory rudder force with axial clearance x_o which was noted in Reference 1 is still evident here, whether thickness effects are included or omitted, although the crests and troughs may shift with change in rudder angle. This periodic variation is confirmed by experimental observations.[10,16]

As can be seen from Figure 9 and Tables 3c, 4c and 5c, the unsteady rudder force is not symmetrical with respect to rudder angle from port to starboard. The difference between port and starboard forces depends very much on the axial clearance between propeller and rudder. At $x_o=0.56r_o$, the change from 0.3 radian to port to 0.3 radian to starboard is -71%, at $x_o=0.72r_o$ it is +124%, and at $x_o=0.8356r_o$ it is -23%.

Calculations have also been performed for a configuration of the same hull and rudder but with a propeller differing from the designed propeller only in that its thickness is doubled. Comparison of the results of these calculations (Tables 6a and 6b) with those for basic thickness show that the effect of doubling the thickness varies from negligible to small (3%) for all steady and unsteady hydrodynamic propeller forces and moments. The steady rudder force and rudder-stock moments are insensitive to propeller thickness. On the other hand, unsteady rudder forces are increased considerably at both design axial clearance and the smallest clearance, as can be seen by a comparison of Table 6b with 3c and 5c.

CONCLUSIONS

The previous study of the hydrodynamic interference between a marine propeller and a rudder, when both lifting surfaces assumed to have no thickness are immersed in a nonuniform flow field, has been modified to include the finite thickness of both interacting surfaces.

Before embarking on the investigation of thickness effects, however, an improvement was sought and achieved in the numerical evaluation of the finite contribution of the singularity in the cross-coupling term K_{PR} which represents the interference effect of propeller on rudder. The results have shown small to moderate effects on the previously determined propeller bearing forces and moments, negligible effects on the steady rudder side force and rudder-stock moment, but large changes in the unsteady rudder force and moment. These latter changes have brought the vibratory values into better agreement with observations.

The propeller thickness contribution to propeller loading which occurs because of its "nonplanar" form is very small provided the thickness is not excessively high.[11] On the other hand, the thickness of its approximated "planar" form produces a "flow distortion" which affects the pressure and velocity fields in the neighborhood of the operating propeller. The former effect, being small and requiring high accuracy to determine, and a more sophisticated mathematical model,[12] has been neglected, whereas the latter effect has been treated in the analysis of the propeller-rudder interaction problem by means of the "thin body" approximation. By a similar approximation the thickness of the rudder is taken into account. Each lifting surface induces some change in the onset velocity distribution on the other.

Expressions have been developed for the normal velocity on each lifting surface due to the thickness of the other and thus a new resultant onset velocity due to both loading and thickness effects is determined and incorporated in the iterative process previously developed.[1]

It is seen that propeller thickness affects only the blade-frequency velocity (and multiples thereof) on the rudder whereas rudder thickness affects all the frequency constituents of the propeller onset velocity (shaft frequency and multiples thereof).

The limited number of calculations have shown that thickness of both lifting surfaces does not change the qualitative description of the results obtained with loading effects alone. The interaction problem is governed mainly by its loading effects.

The values of mean thrust and torque are changed 0.8 to 1.1% by the inclusion of thickness of both lifting surfaces, the corresponding vibratory values by 2 to 5%, the maximum changes occurring at the smallest axial clearance between propeller and rudder. The effect of thickness on the propeller bearing forces and moments is almost independent of rudder angle and diminishes with increase in axial clearance. The steady-state rudder force and rudder-stock moment are hardly affected by the inclusion of propeller and rudder thickness. However, the effect of thickness can be large in the case of unsteady rudder lateral force and rudder-stock moment and varies cyclically with axial clearance. The observation that the blade-frequency rudder force varies periodically with axial clearance is valid whether or not thickness effects are included.

The numerical procedure for evaluating the steady-state and unsteady loading distributions and corresponding hydrodynamic forces and moments on both lifting surfaces due to thickness and loading effects is adapted to the CDC 6600 high-speed digital computer. Inclusion of thickness effects has increased computer running time by only 10%.

With the improved program and inclusion of thickness effects, it is now advisable to perform a systematic series of calculations to bring out the roles of various parameters, such as number, expanded area ratio and thickness of propeller blades, aspect ratio and thickness of rudder, etc., in the propeller-rudder interaction, in the search for the optimum propeller-rudder configuration.

REFERENCES

1. S. Tsakonas, W.R. Jacobs and M.R. Ali, "A Theory for the Propeller-Rudder Interaction," Report SIT-DL-68-1284, Stevens Institute of Technology, August 1968; published as "Application of the Unsteady-Lifting-Surface Theory to the Study of Propeller-Rudder Interaction," J. Ship Research, Vol. 14, No. 3, September 1970, pp 181-194.

2. J. Shioiri and S. Tsakonas, "Three-Dimensional Approach to the Gust Problem for a Screw Propeller," DL Report 940, Stevens Institute of Technology, March 1963; J. Ship Research, Vol. 7, No. 4, April 1964, pp 29-53.

3. S. Tsakonas and W.R. Jacobs, "Unsteady Lifting Surface Theory for a Marine Propeller of Low Pitch Angle with Chordwise Loading Distribution," DL Report 994, Stevens Institute of Technology, January 1964; J. Ship Research, Vol. 9, No. 2, September 1965, pp 79-101.

4. S. Tsakonas, C.Y. Chen and W.R. Jacobs, "Exact Treatment of the Helicoidal Wake in the Propeller Lifting-Surface Theory," DL Report 1117, Stevens Institute of Technology, August 1966; J. Ship Research, Vol. 11, No. 3, September 1967, pp 154-170.

5. S. Tsakonas, W.R. Jacobs and P.H. Rank, "Unsteady Propeller Lifting-Surface Theory with Finite Number of Chordwise Modes," DL Report 1133, December 1966; J. Ship Research, Vol. 12, No. 1, March 1968, pp 14-46.

6. S. Tsakonas and W.R. Jacobs, "Propeller Loading Distributions," DL Report 1319, Stevens Institute of Technology, August 1968; J. Ship Research, Vol. 13, No. 3, December 1969, pp 237-257.

7. W.R. Jacobs and S. Tsakonas, "Generalized Lift Operator Technique for the Solution of the Downwash Integral Equation," DL Report 1308, Stevens Institute of Technology, August 1968; published as "A New Procedure for the Solution of Lifting Surface Problems," J. Hydronautics, Vol. 3, No. 1, January 1969, pp 20-28.

8. M. Lotveit, "A Study of Rudder Action with Special Reference to Single-Screw Ships," North East Coast Institute of Engineers and Shipbuilders, Vol. 73, 1959.

9. A.F. Lehman, and R. Romandetto, "An Experimental Study of the Unsteady Forces Induced on a Rudder due to a Propeller Acting in a Wake," Oceanics, Inc. Report No. 68-58, December 1968.

10. F.M. Lewis, "Propeller Vibretion Forces in Single Screw Ships," Trans. SNAME, Vol. 77, 1969.

11. W.R. Jacobs and S. Tsakonas, "Blade Thickness Effects on Propeller Loading," Stevens Institute of Technology Report SIT-DL-72-1629 (in preparation).

12. S. Tsakonas, W.R. Jacobs and M.R. Ali, "An Exact Linear Lifting-Surface Theory for a Marine Propeller in a Nonuniform Flow Field," Stevens Institute of Technology Report SIT-DL-72-1509, February 1972.

13. W.R. Jacobs and S. Tsakonas, "Propeller-Induced Velocity Field by Means of Unsteady Lifting Surface Theory," Stevens Institute of Technology Report SIT-DL-72-1588, February 1972.

14. J.P. Breslin and S. Tsakonas, "Marine Propeller Pressure Field due to Loading and Thickness Effect," Transactions SNAME, Vol. 67, 1959.

15. W.R. Jacobs, J. Mercier and S. Tsakonas, "Theory and Measurements of the Propeller-Induced Vibratory Field," Stevens Institute of Technology Report SIT-DL-70-1485, December 1970; J. Ship Research, Vol. 16, No. 2, June 1972, pp 124-139.

16. K. Sugai, "On Vibratory Forces Induced on the Rudder Behind a Propeller," Ship Research Institute, Tokyo; presented at Spring Meeting of S.N.A. in Japan, May 1964.

TABLE 1

MEAN FORCE AND MOMENT COEFFICIENTS
(Without Thickness Effects)

Comparison Of Results Of The Modified Program (1972)
With Those Of Reference 1

Amplitudes	Rudder Angle (rad)	$x_o=0.8356r_o$ Ref.1	$x_o=0.8356r_o$ 1972	$x_o=0.72r_o$ Ref.1	$x_o=0.72r_o$ 1972	$x_o=0.56r_o$ Ref.1	$x_o=0.56r_o$ 1972
$\bar{K}_{F_x}=\bar{K}_T$	-0.3	.3737	.3738	.3738	.3743	.3737	.3738
	0	.3737	.3738	.3738	.3743	.3737	.3738
	0.3	.3737	.3738	.3738	.3743	.3737	.3738
$\bar{K}_{Q_x}=\bar{K}_Q$	-0.3	.0648	.0648	.0648	.0648	.0648	.0648
	0	.0648	.0648	.0648	.0648	.0648	.0648
	0.3	.0648	.0648	.0648	.0648	.0648	.0648
$^*\bar{K}_{F_y}$	-0.3	.00659	.00574	.00772	.00640	.00868	.00779
	0	.00254	.00275	.00254	.00261	.00235	.00264
	0.3	.00151	.00024	.00263	.00117	.00398	.00250
$^*\bar{K}_{Q_y}$	-0.3	.00028	.00001	.00060	.00019	.00059	.00067
	0	.00143	.00135	.00145	.00149	.00152	.00141
	0.3	.00315	.00271	.00350	.00317	.00362	.00348
$^*\bar{K}_{F_z}$	-0.3	.00378	.00122	.00660	.00304	.01362	.00672
	0	.00342	.00339	.00345	.00325	.00327	.00319
	0.3	.01062	.00800	.01351	.00955	.02010	.01311
$^*\bar{K}_{Q_z}$	-0.3	.00062	.00065	.00195	.00040	.00476	.00218
	0	.00367	.00363	.00368	.00353	.00364	.00353
	0.3	.00795	.00662	.00931	.00745	.01204	.00924
$\bar{C}_{F_R}$	-0.3	1.032	1.045	1.039	1.048	1.046	1.055
	0	.026	.033	.026	.034	.027	.034
	0.3	1.032	1.006	1.035	1.009	1.047	1.015
$\bar{C}_{M_R}$	-0.3	.0690	.0697	.0692	.0698	.0685	.0697
	0	.0018	.0022	.0019	.0023	.0018	.0023
	0.3	.0695	.0675	.0698	.0677	.0692	.0679

$$K_F = \frac{F}{\rho_f n^2 D^4}\ ,\quad K_Q = \frac{Q}{\rho_f n^2 D^5}\ ,\quad C_{F_R} = \frac{F_R}{\frac{\rho_f}{2} A_R U^2}\ ,\quad C_{M_R} = \frac{M_R}{\frac{\rho_f}{2} A_R U^2 (2C_R)}$$

*corrected mean values for Reference 1

TABLE 2

BLADE FREQUENCY FORCE AND MOMENT COEFFICIENTS
(Without Thickness Effects)

Comparison Of Results Of The Modified Program (1972)
With Those Of Reference 1

Amplitudes	Rudder Angle (rad)	$x_o=0.8356r_o$		$x_o=0.72r_o$		$x_o=0.56r_o$	
		Ref.1	1972	Ref.1	1972	Ref.1	1972
$\tilde{K}_{F_x}$	-0.3	.0120	.0120	.0119	.0126	.0108	.0119
	0	.0120	.0121	.0119	.0126	.0111	.0119
	0.3	.0120	.0125	.0119	.0126	.0117	.0119
$\tilde{K}_{Q_x}$	-0.3	.00210	.00210	.00207	.00220	.00190	.00208
	0	.00210	.00211	.00208	.00220	.00194	.00208
	0.3	.00210	.00212	.00208	.00220	.00205	.00208
$\tilde{K}_{F_y}$	-0.3	.00350	.00280	.00462	.00309	.00911	.00455
	0	.00252	.00250	.00246	.00249	.00278	.00254
	0.3	.00212	.00230	.00277	.00221	.00782	.00280
$\tilde{K}_{Q_y}$	-0.3	.00246	.00212	.00303	.00226	.00524	.00292
	0	.00200	.00200	.00198	.00205	.00189	.00199
	0.3	.00200	.00196	.00244	.00202	.00498	.00240
$\tilde{K}_{F_z}$	-0.3	.00299	.00283	.00314	.00309	.00422	.00312
	0	.00279	.00273	.00273	.00292	.00269	.00275
	0.3	.00285	.00270	.00306	.00290	.00409	.00307
$\tilde{K}_{Q_z}$	-0.3	.00231	.00225	.00235	.00240	.00263	.00238
	0	.00224	.00221	.00221	.00234	.00226	.00223
	0.3	.00230	.00221	.00239	.00236	.00268	.00233
$\tilde{C}_{F_R}$	-0.3	.0745	.0152	.0639	.0182	.1048	.0027
	0	.0440	.0174	.0365	.0132	.0544	.0109
	0.3	.0508	.0213	.0429	.0082	.0617	.0233
$\tilde{C}_{M_R}$	-0.3	.0200	.00223	.0281	.00277	.0363	.00389
	0	.0122	.00245	.0145	.00352	.0133	.00306
	0.3	.0125	.00275	.0156	.00446	.0204	.00322

TABLE 3a

MEAN PROPELLER FORCE AND MOMENT COEFFICIENTS
(With And Without Thickness Effects)

$x_o = 0.8356 r_o$

Coeff.	Thickness	Rudder Angle In Radians						
		-.3	-.2	-.1	0	.1	.2	.3
$\bar{K}_T$	t	-.3707	-.3707	-.3707	-.3707	-.3707	-.3707	-.3707
	0	-.3738	-.3738	-.3738	-.3738	-.3738	-.3738	-.3738
$\bar{K}_Q$	t	.0643	.0643	.0643	.0643	.0643	.0643	.0643
	0	.0648	.0648	.0648	.0648	.0648	.0648	.0648
$\bar{K}_{F_y}$	t	.00478	.00378	.00279	.00179	.00080	-.00020	-.00119
	0	.00574	.00474	.00374	.00275	.00175	.00076	-.00024
$\bar{K}_{Q_y}$	t	-.00056	-.00102	-.00147	-.00192	-.00238	-.00283	-.00328
	0	.00001	-.00044	-.00090	-.00135	-.00180	-.00226	-.00271
$\bar{K}_{F_z}$	t	.00164	.00011	-.00143	-.00296	-.00450	-.00600	-.00757
	0	.00122	-.00032	-.00185	-.00339	-.00493	-.00640	-.00800
$\bar{K}_{Q_z}$	t	-.00048	-.00147	-.00250	-.00346	-.00446	-.00546	-.00645
	0	-.00065	-.00164	-.00264	-.00363	-.00463	-.00563	-.00662

NOTE: t designates values with thickness effects

0 without thickness effects

negative rudder angles are to starboard

TABLE 3b

BLADE-FREQUENCY PROPELLER FORCE AND MOMENT COEFFICIENTS
(With And Without Thickness Effects)

$x_o = 0.8356 r_o$

Coeff.	Thickness		Rudder Angle In Radians -.3	-.2	-.1	0	.1	.2	.3
$\tilde{K}_{F_x}$	t	Mag.	.0118	.0118	.0119	.0119	.0119	.0119	.0119
		Phase^o	203	203	203	202	202	202	202
	0	M	.0120	.0121	.0121	.0121	.0121	.0121	.0121
		P	203	203	203	202	202	202	202
$\tilde{K}_{Q_x}$	t	M	.00207	.00207	.00207	.00207	.00208	.00208	.00208
		P	23	23	23	22	22	22	22
	0	M	.00210	.00210	.00211	.00211	.00211	.00211	.00212
		P	23	23	23	22	22	22	22
$\tilde{K}_{F_y}$	t	M	.00260	.00254	.00252	.00251	.00252	.00254	.00257
		P	158	164	168	172	176	180	183
	0	M	.00280	.00269	.00259	.00250	.00243	.00236	.00230
		P	163	166	169	173	177	181	185
$\tilde{K}_{Q_y}$	t	M	.00203	.00198	.00194	.00191	.00188	.00187	.00186
		P	-5	-2	2	6	10	14	18
	0	M	.00212	.00207	.00204	.00200	.00198	.00197	.00196
		P	-4	-1	3	6	10	14	18
$\tilde{K}_{F_z}$	t	M	.00283	.00273	.00261	.00251	.00242	.00235	.00300
		P	106	111	115	119	123	128	121
	0	M	.00283	.00279	.00276	.00273	.00272	.00271	.00270
		P	108	111	114	117	120	123	126
$\tilde{K}_{Q_z}$	t	M	.00218	.00217	.00215	.00215	.00214	.00214	.00215
		P	-71	-69	-66	-64	-61	-59	-56
	0	M	.00225	.00224	.00222	.00221	.00221	.00221	.00221
		P	-71	-69	-66	-64	-62	-59	-57

TABLE 3c

MEAN AND BLADE-FREQUENCY RUDDER FORCE AND MOMENT COEFFICIENTS
(With And Without Thickness Effects)

$x_o = 0.8356 r_o$

Coeff.	Thickness		Rudder Angle In Radians -.3	-.2	-.1	0	.1	.2	.3
MEAN									
$\tilde{C}_{F_R}$	t	Mag.	1.039	0.698	0.356	0.031	0.330	0.671	1.012
		Phase°	177	176	174	114	3	1	0
	0	M	1.045	0.704	0.362	0.032	0.323	0.664	1.006
		P	177	176	174	125	3	1	0
$\tilde{C}_{M_R}$	t	M	.0695	.0466	.0237	.00212	.0224	.0452	.0682
		P	177	176	173	107	3	1	0
	0	M	.0697	.0469	.0240	.00219	.0218	.0447	.0675
		P	177	176	174	118	3	1	0
BLADE-FREQUENCY									
$\tilde{C}_{F_R}$	t	M	.0222	.0229	.0238	.0248	.0260	.0273	.0287
		P	-44	-49	-54	-59	-63	-66	-69
	0	M	.0152	.0157	.0164	.0174	.0185	.0198	.0213
		P	-36	-44	-51	-57	-63	-68	-72
$\tilde{C}_{M_R}$	t	M	.00236	.00244	.00252	.00261	.00271	.00282	.00293
		P	-45	-41	-37	-34	-31	-28	-25
	0	M	.00223	.00229	.00236	.00245	.00254	.00264	.00275
		P	-49	-45	-41	-37	-34	-30	-28

TABLE 4a

MEAN PROPELLER FORCE AND MOMENT COEFFICIENTS
(With And Without Thickness Effects)

$x_o = 0.72r_o$

Coeff.	Thickness	Rudder Angle In Radians -.3	-.2	-.1	0	.1	.2	.3
$\bar{K}_T$	t	-.3705	-.3705	-.3705	-.3705	-.3705	-.3705	-.3705
	0	-.3743	-.3743	-.3743	-.3743	-.3743	-.3743	-.3743
$\bar{K}_Q$	t	.0642	.0642	.0642	.0642	.0642	.0642	.0642
	0	.0648	.0648	.0648	.0648	.0648	.0648	.0648
$\bar{K}_{F_y}$	t	.00505	.00379	.00253	.00127	.00001	-.00125	-.00251
	0	.00640	.00514	.00388	.00261	.00135	.00009	-.00117
$\bar{K}_{Q_y}$	t	-.00060	-.00116	-.00171	-.00227	-.00283	-.00339	-.00395
	0	.00019	-.00037	-.00093	-.00149	-.00205	-.00261	-.00317
$\bar{K}_{F_z}$	t	.00369	.00159	-.00050	-.00260	-.00470	-.00680	-.00890
	0	.00304	.00094	-.00115	-.00325	-.00535	-.00745	-.00955
$\bar{K}_{Q_z}$	t	.00067	-.00064	-.00195	-.00326	-.00456	-.00587	-.00718
	0	.00040	-.00091	-.00222	-.00353	-.00483	-.00614	-.00745

NOTE: t designates values with thickness effects
0 without thickness effects
negative rudder angles are to starboard

TABLE 4b

BLADE-FREQUENCY PROPELLER FORCE AND MOMENT COEFFICIENTS
(With And Without Thickness Effects)

$x_o = 0.72r_o$

Coeff.	Thickness		Rudder Angle In Radians						
			-.3	-.2	-.1	0	.1	.2	.3
$\tilde{K}_{F_x}$	t	Mag.	.0121	.0121	.0121	.0121	.0121	.0121	.0121
		Phase°	208	208	208	207	207	206	206
	0	M	.0126	.0126	.0126	.0126	.0126	.0126	.0126
		P	208	208	207	207	206	206	206
$\tilde{K}_{Q_x}$	t	M	.00211	.00211	.00211	.00211	.00212	.00212	.00212
		P	28	28	28	27	27	26	26
	0	M	.00220	.00220	.00220	.00220	.00220	.00220	.00220
		P	28	28	27	27	26	26	26
$\tilde{K}_{F_y}$	t	M	.00287	.00263	.00240	.00221	.00206	.00195	.00190
		P	153	158	164	171	179	188	198
	0	M	.00309	.00287	.00266	.00249	.00242	.00226	.00221
		P	158	162	168	174	182	190	198
$\tilde{K}_{Q_y}$	t	M	.00209	.00197	.00189	.00182	.00179	.00178	.00181
		P	-11	-5	2	9	16	23	31
	0	M	.00226	.00216	.00208	.00205	.00199	.00199	.00202
		P	-4	-3	4	10	17	23	30
$\tilde{K}_{F_z}$	t	M	.00293	.00286	.00280	.00275	.00273	.00272	.00274
		P	103	107	112	116	121	126	131
	0	M	.00309	.00302	.00296	.00292	.00290	.00289	.00290
		P	104	108	112	117	121	126	130
$\tilde{K}_{Q_z}$	t	M	.00230	.00227	.00225	.00224	.00223	.00224	.00226
		P	-74	-70	-67	-63	-59	-55	-52
	0	M	.00240	.00237	.00235	.00234	.00234	.00235	.00236
		P	-73	-70	-66	-63	-59	-56	-52

TABLE 4c

MEAN AND BLADE-FREQUENCY RUDDER FORCE AND MOMENT COEFFICIENTS
(With And Without Thickness Effects)

$x_o = 0.72r_o$

Coeff.	Thickness		Rudder Angle In Radians -.3	-.2	-.1	0	.1	.2	.3
MEAN									
$\bar{C}_{F_R}$	t	Mag.	1.039	0.696	0.354	0.032	0.334	0.676	1.019
		Phase°	176	175	172	106	3	0	0
	0	M	1.048	0.706	0.364	0.034	0.324	0.666	1.009
		P	176	175	173	123	2	0	-1
$\bar{C}_{M_R}$	t	M	.0692	.0463	.0234	.00225	.0226	.0455	.0684
		P	176	175	172	97	3	0	0
	0	M	.0698	.0469	.0241	.00229	.0219	.0448	.0677
		P	176	175	173	115	3	0	-1
BLADE-FREQUENCY									
$\tilde{C}_{F_R}$	t	M	.0179	.0163	.0146	.0130	.0113	.0096	.0080
		P	125	124	124	123	122	121	119
	0	M	.0182	.0165	.0149	.0132	.0115	.0098	.0082
		P	132	132	133	133	134	135	136
$\tilde{C}_{M_R}$	t	M	.00278	.00300	.00325	.00353	.00383	.00415	.00447
		P	-111	-117	-123	-127	-131	-134	-137
	0	M	.00277	.00299	.00325	.00352	.00382	.00414	.00446
		P	-111	-117	-123	-127	-131	-134	-137

TABLE 5a

MEAN PROPELLER FORCE AND MOMENT COEFFICIENTS
(With And Without Thickness Effects)

$x_o = 0.56r_o$

Coeff.	Thickness	Rudder Angle in Radians -.3	-.2	-.1	0	.1	.2	.3
$\bar{K}_T$	t	-.3696	-.3696	-.3696	-.3696	-.3696	-.3696	-.3696
	0	-.3738	-.3738	-.3738	-.3738	-.3738	-.3738	-.3738
$\bar{K}_Q$	t	.0641	.0641	.0641	.0641	.0641	.0641	.0641
	0	.0648	.0648	.0648	.0648	.0648	.0648	.0648
$\bar{K}_{F_y}$	t	.00542	.00370	.00197	.00025	-.00148	-.00320	-.00492
	0	.00779	.00607	.00436	.00264	.00093	-.00078	-.00250
$\bar{K}_{Q_y}$	t	-.00065	-.00136	-.00206	-.00277	-.00347	-.00417	-.00488
	0	.00067	-.00002	-.00072	-.00141	-.00210	-.00279	-.00348
$\bar{K}_{F_z}$	t	.00768	.00434	.00104	-.00228	-.00560	-.00892	-.01224
	0	.00672	.00342	.00011	-.00319	-.00650	-.00980	-.01311
$\bar{K}_{Q_z}$	t	.00262	.00069	-.00122	-.00314	-.00506	-.00698	-.00890
	0	.00218	.00028	-.00162	-.00353	-.00543	-.00734	-.00924

NOTE: t designates values with thickness effects
0 without thickness effects
negative rudder angles are to starboard

TABLE 5b

BLADE-FREQUENCY PROPELLER FORCE AND MOMENT COEFFICIENTS
(With And Without Thickness Effects)

$x_o = 0.56r_o$

Coeff.	Thickness	Mag. / Phase	Rudder Angle In Radians -.3	-.2	-.1	0	.1	.2	.3
$\tilde{K}_{F_x}$	t	Mag.	.0113	.0113	.0113	.0113	.0113	.0112	.0112
		Phase	211	210	209	208	208	207	206
	0	M	.0119	.0119	.0119	.0119	.0119	.0119	.0119
		P	204	203	202	202	201	200	199
$\tilde{K}_{Q_x}$	t	M	.00198	.00198	.00197	.00197	.00197	.00196	.00196
		P	31	30	29	28	28	27	26
	0	M	.00208	.00208	.00208	.00208	.00208	.00208	.00208
		P	24	23	22	22	21	20	19
$\tilde{K}_{F_y}$	t	M	.00402	.00318	.00242	.00182	.00159	.00187	.00249
		P	132	139	150	169	200	230	249
	0	M	.00455	.00377	.00308	.00254	.00228	.00238	.00280
		P	138	145	156	171	193	216	234
$\tilde{K}_{Q_y}$	t	M	.00255	.00211	.00176	.00157	.00159	.00181	.00218
		P	-35	-25	-11	8	30	49	62
	0	M	.00292	.00251	.00219	.00199	.00197	.00211	.00240
		P	-31	-22	-10	5	23	39	52
K_{F_z}	t	M	.00282	.00263	.00251	.00246	.00250	.00262	.00280
		P	91	100	110	120	131	140	149
	0	M	.00312	.00293	.00281	.00275	.00277	.00286	.00307
		P	92	100	109	118	127	136	145
$\tilde{K}_{Q_z}$	t	M	.00224	.00217	.00213	.00211	.00213	.00218	.00225
		P	-81	-75	-68	-61	-55	-48	-41
	0	M	.00238	.00230	.00225	.00223	.00223	.00227	.00233
		P	-83	-77	-71	-64	-58	-51	-45

TABLE 5c

MEAN AND BLADE-FREQUENCY RUDDER FORCE AND MOMENT COEFFICIENTS
(With And Without Thickness Effects)

$x_o = 0.56r_o$

Coeff.	Thickness		Rudder Angle In Radians -.3	-.2	-.1	0	.1	.2	.3
MEAN									
$\bar{C}_{F_R}$	t	Mag.	1.032	0.688	0.344	0.031	0.349	0.693	1.037
		Phase°	173	172	170	80	0	-2	-3
	0	M	1.055	0.710	0.366	0.034	0.326	0.670	1.015
		P	174	173	171	121	0	-2	-3
$\bar{C}_{M_R}$	t	M	.0684	.0455	.0225	.0023	.0237	.0466	.0696
		P	173	172	169	70	0	-2	-3
	0	M	.0697	.0468	.0239	.0023	.0221	.0450	.0679
		P	173	172	170	108	1	-2	-3
BLADE-FREQUENCY									
$\tilde{C}_{F_R}$	t	M	.0096	.0129	.0166	.0205	.0244	.0285	.0326
		P	233	220	212	208	205	202	200
	0	M	.0027	.0031	.0068	.0109	.0150	.0191	.0233
		P	322	229	206	200	197	195	194
$\tilde{C}_{M_R}$	t	M	.00443	.00414	.00392	.00378	.00374	.00379	.00394
		P	100	93	85	76	67	58	49
	0	M	.00389	.00353	.00325	.00306	.00299	.00305	.00322
		P	106	99	90	79	67	56	45

TABLE 6a

MEAN PROPELLER AND RUDDER FORCE AND MOMENT COEFFICIENTS WITH PROPELLER OF DOUBLE THICKNESS

Coefficient	Rudder Angle rad	Axial Clearance x_o/r_o 0.56	0.8356
$\bar{K}_T$	-0.3(stbd)	0.3690	0.3707
	0	0.3690	0.3707
	0.3(port)	0.3690	0.3707
$\bar{K}_Q$	-0.3	0.0640	0.0643
	0	0.0640	0.0643
	0.3	0.0640	0.0643
$\bar{K}_{F_y}$	-0.3	0.0055	0.0048
	0	0.0003	0.0018
	0.3	-0.0048	-0.0012
$\bar{K}_{Q_y}$	-0.3	-0.0006	-0.0006
	0	-0.0026	-0.0019
	0.3	-0.0047	-0.0033
$\bar{K}_{F_z}$	-0.3	0.0074	0.0016
	0	-0.0026	-0.0030
	0.3	-0.0125	-0.0076
$\bar{K}_{Q_z}$	-0.3	0.0024	-0.0005
	0	-0.0033	-0.0035
	0.3	-0.0091	-0.0065
$\bar{C}_{F_R}$	-0.3	1.033	1.039
	0	0.028	0.031
	0.3	1.037	1.012
$\bar{C}_{M_R}$	-0.3	0.682	0.0693
	0	0.0021	0.0021
	0.3	0.0693	0.0679

TABLE 6b

BLADE-FREQUENCY PROPELLER AND RUDDER FORCE AND MOMENT COEFFICIENTS WITH PROPELLER OF DOUBLE THICKNESS

Amplitude	Rudder Angle rad	Axial Clearance x_o/r_o 0.56	0.8356
$\tilde{K}_{F_x}$	-0.3(stbd)	0.0109	0.0118
	0	0.0108	0.0119
	0.3(port)	0.0108	0.0119
$\tilde{K}_{Q_x}$	-0.3	0.0019	0.0021
	0	0.0019	0.0021
	0.3	0.0019	0.0021
$\tilde{K}_{F_y}$	-0.3	0.0040	0.0027
	0	0.0018	0.0024
	0.3	0.0025	0.0022
$\tilde{K}_{Q_y}$	-0.3	0.0025	0.0020
	0	0.0015	0.0019
	0.3	0.0022	0.0019
$\tilde{K}_{F_z}$	-0.3	0.0027	0.0027
	0	0.0024	0.0026
	0.3	0.0027	0.0026
$\tilde{K}_{Q_z}$	-0.3	0.0022	0.0022
	0	0.0020	0.0021
	0.3	0.0022	0.0021
$\tilde{C}_{F_R}$	-0.3	0.0210	0.0287
	0	0.0316	0.0317
	0.3	0.0431	0.0355
$\tilde{C}_{M_R}$	-0.3	0.0034	0.0026
	0	0.0033	0.0029
	0.3	0.0041	0.0032

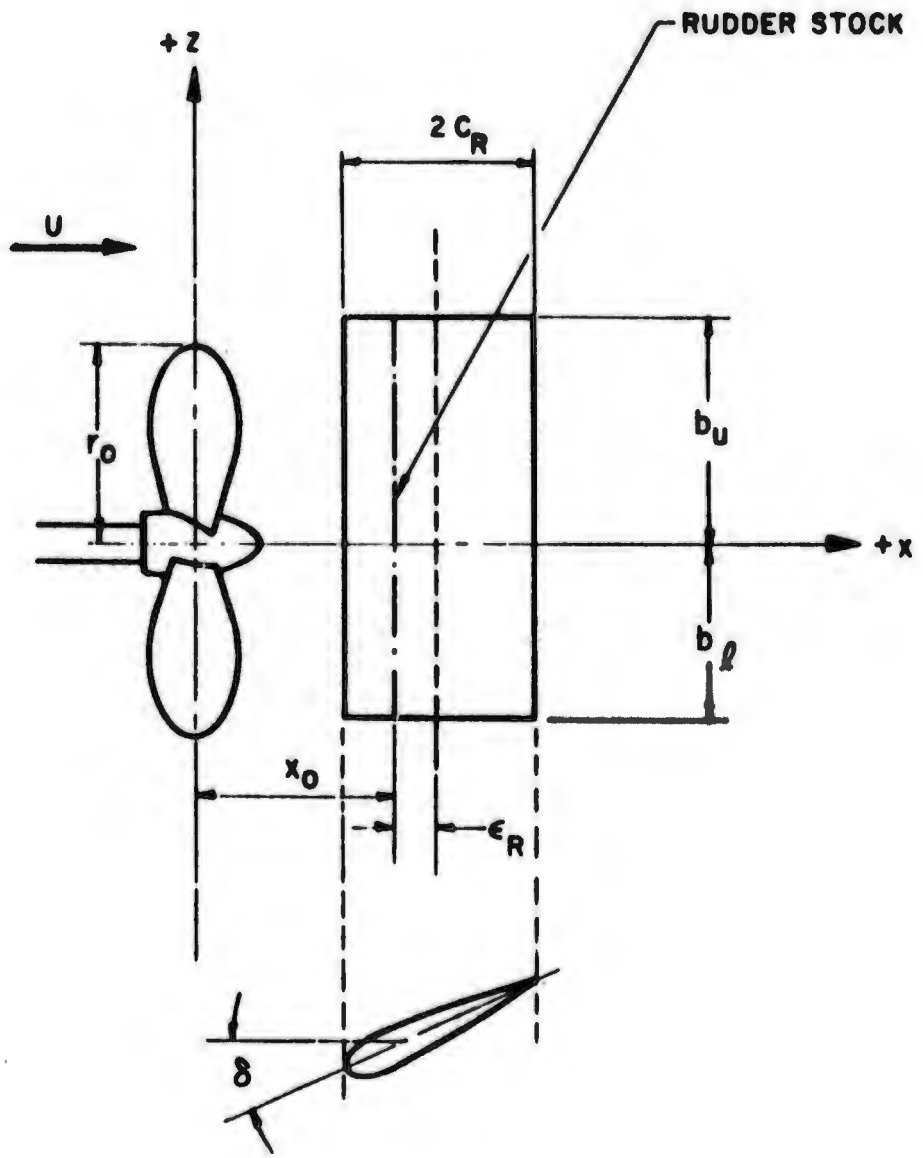

FIG. 1. PROPELLER - RUDDER ARRANGEMENT

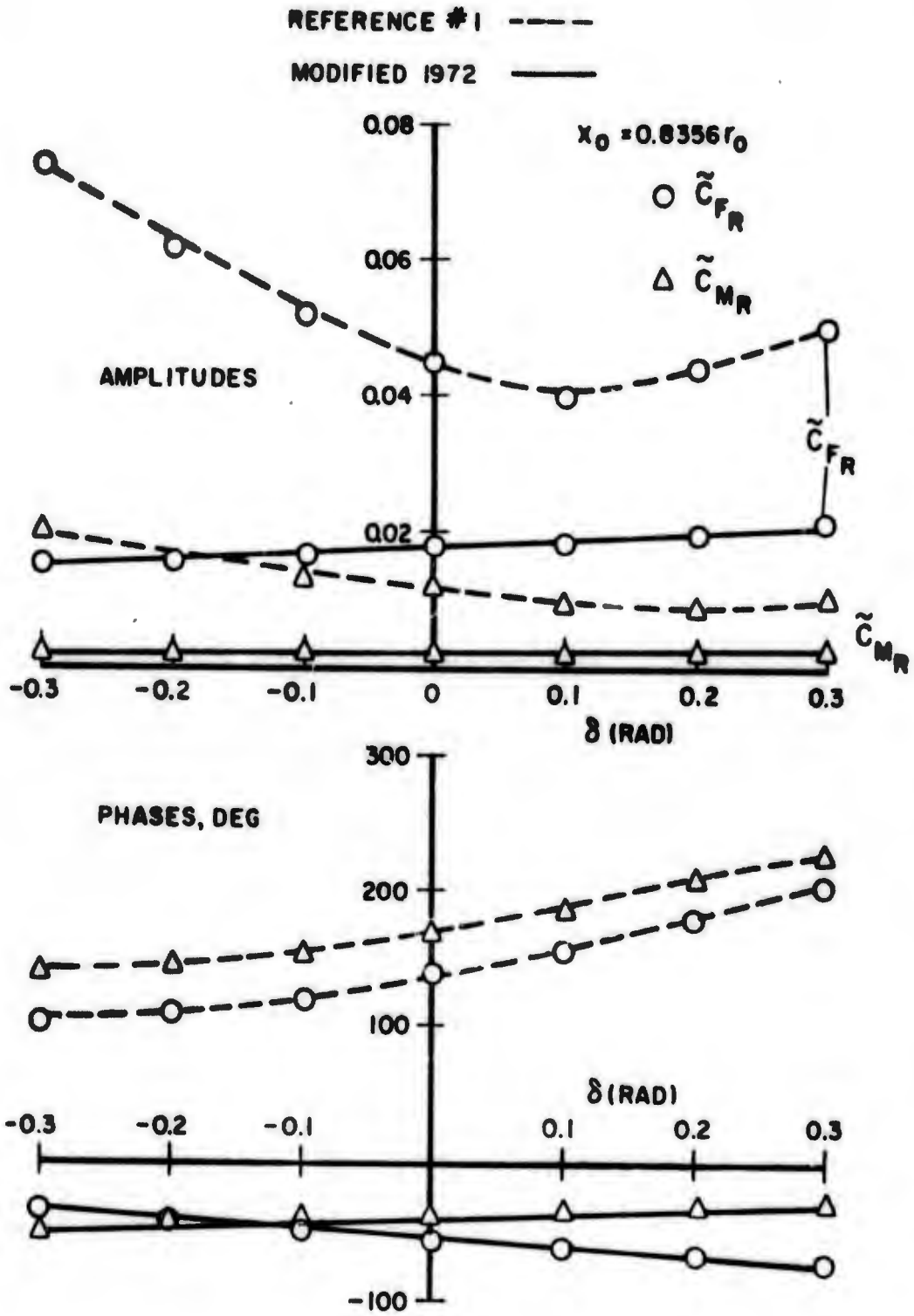

FIG.2 BLADE-FREQUENCY RUDDER LATERAL FORCE AND RUDDER STOCK MOMENT COEFFICIENTS VERSUS RUDDER ANGLE

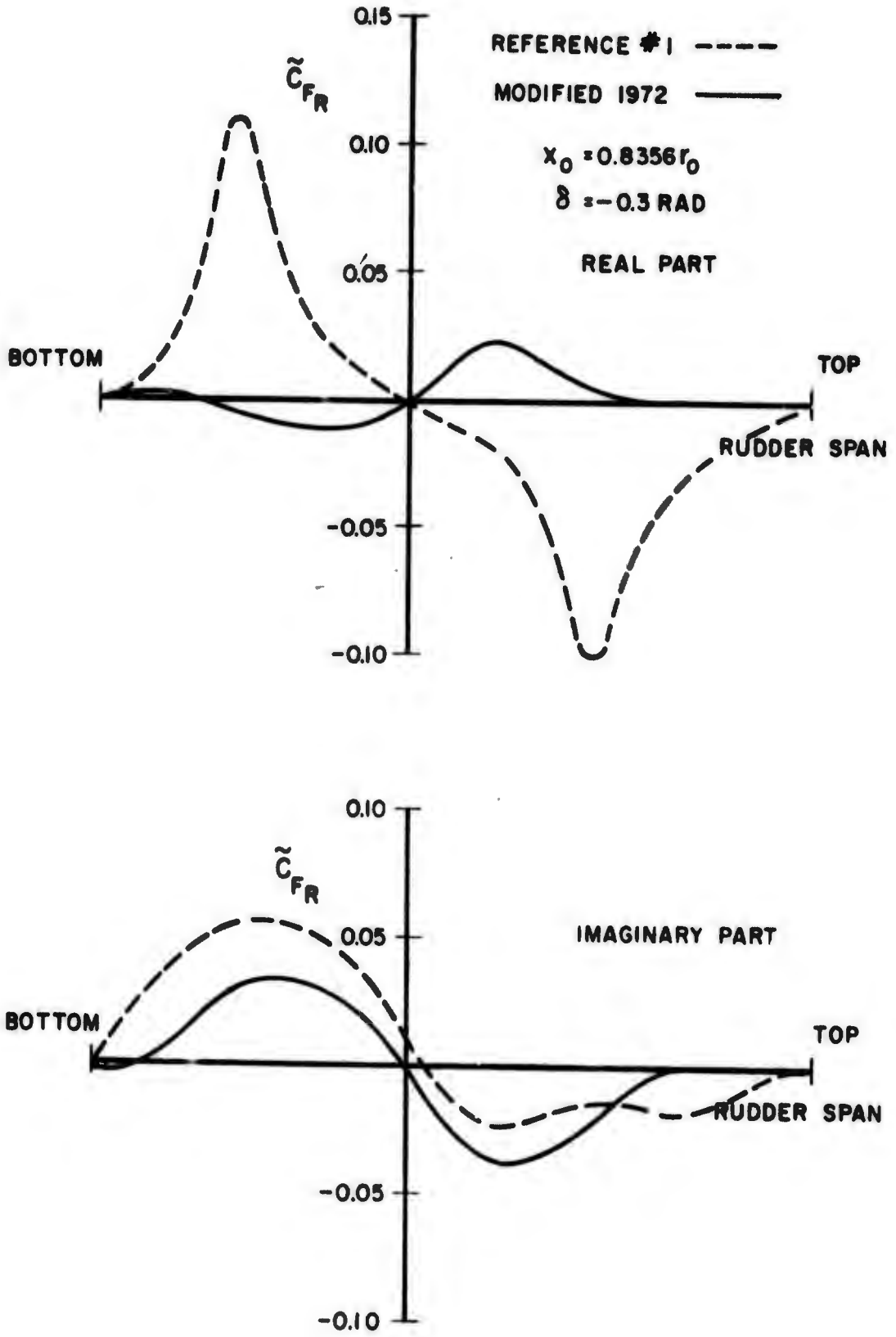

FIG. 3. SPANWISE DISTRIBUTION OF BLADE FREQUENCY $\tilde{C}_{F_R}$ FOR RUDDER ANGLE OF 0.3 RADIAN TO STARBOARD, AND RUDDER LOCATION $X_0 = 0.8356\, r_0$

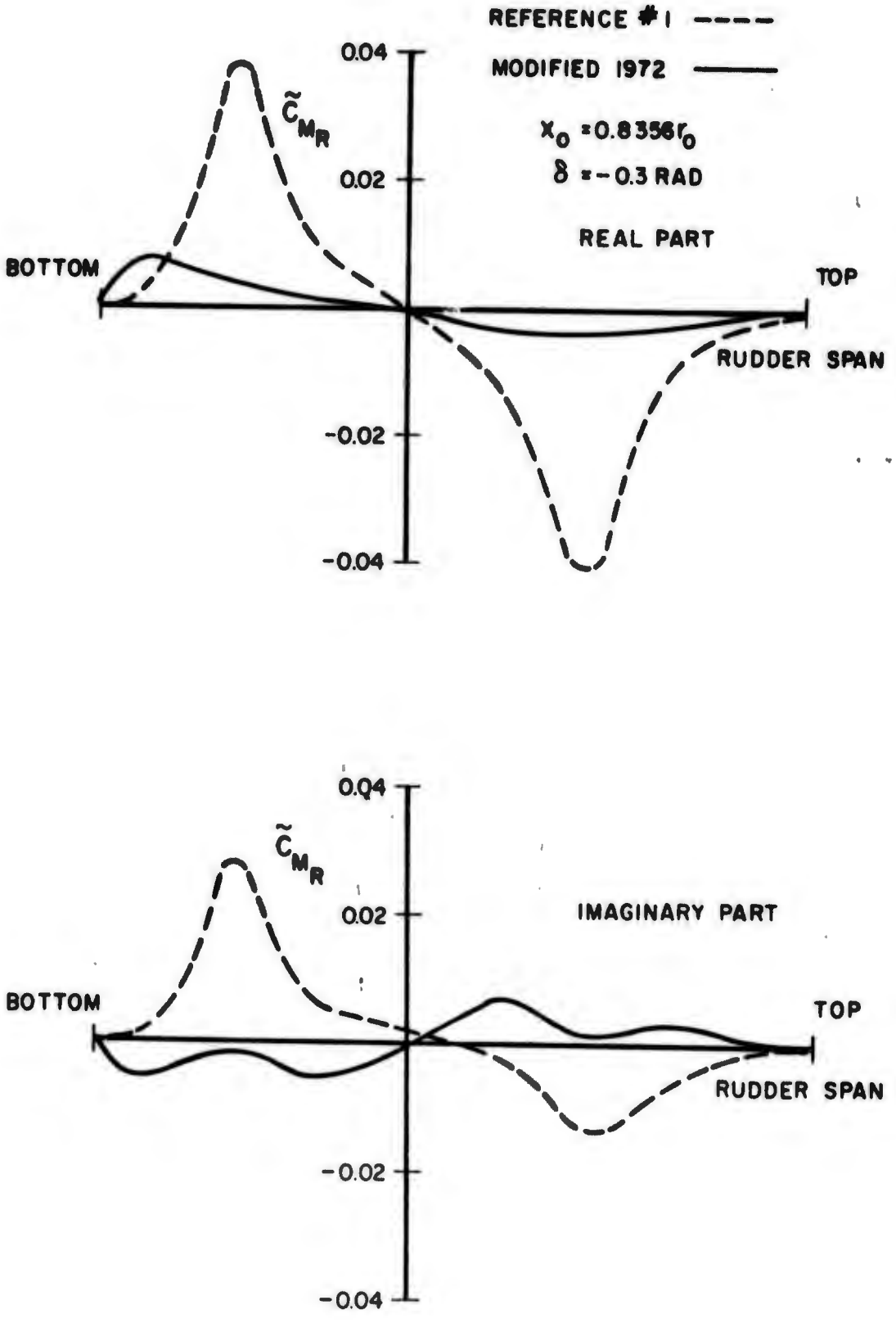

FIG. 4. SPANWISE DISTRIBUTION OF BLADE FREQUENCY $\tilde{C}_{M_R}$ FOR RUDDER ANGLE OF 0.3 RADIAN TO STARBOARD, AND RUDDER LOCATION $X_0 = 0.8356 r_0$

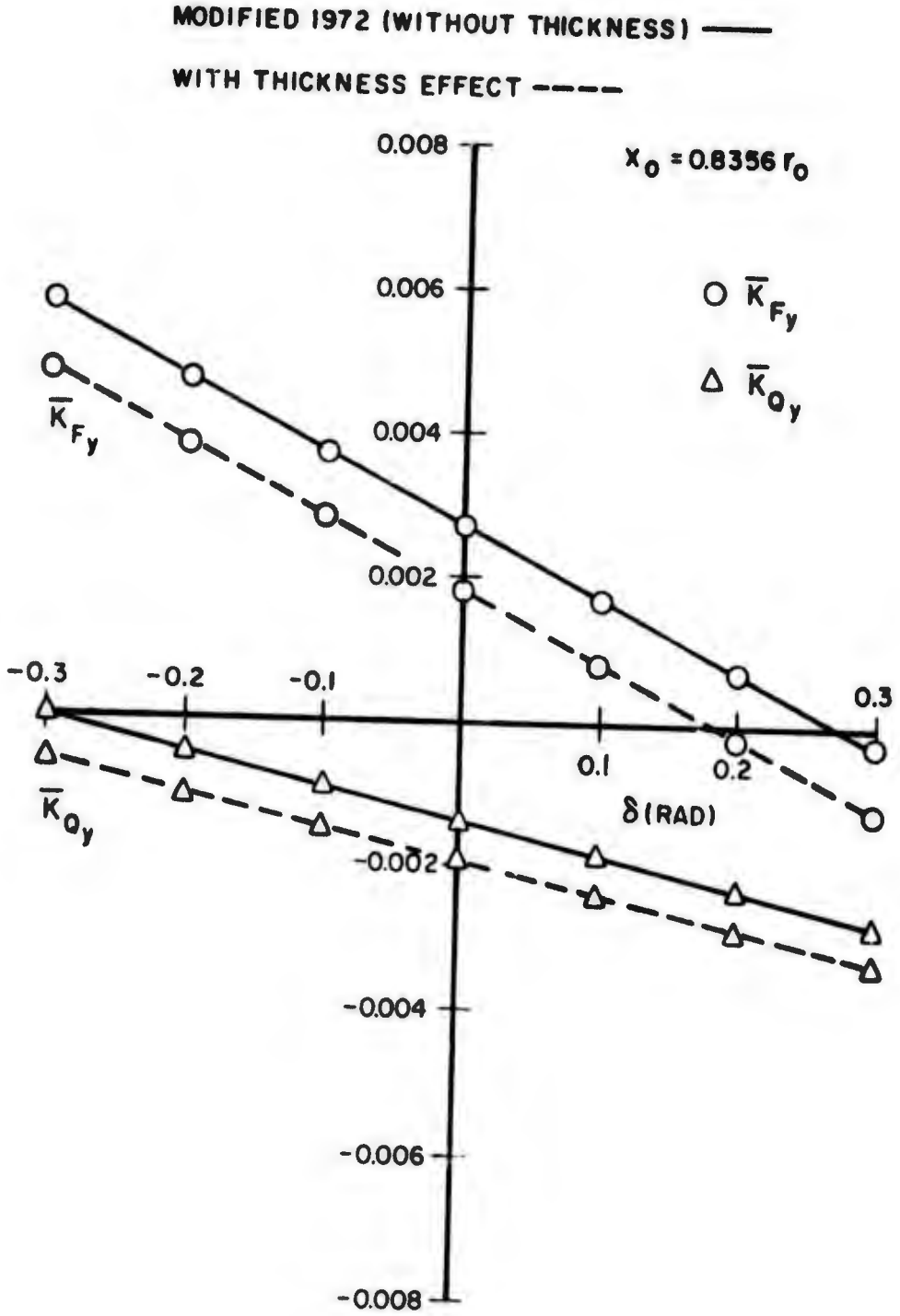

FIG. 5. MEAN HORIZONTAL BEARING FORCE AND BENDING MOMENT COEFFICIENTS ABOUT Y-AXIS VERSUS RUDDER ANGLE δ

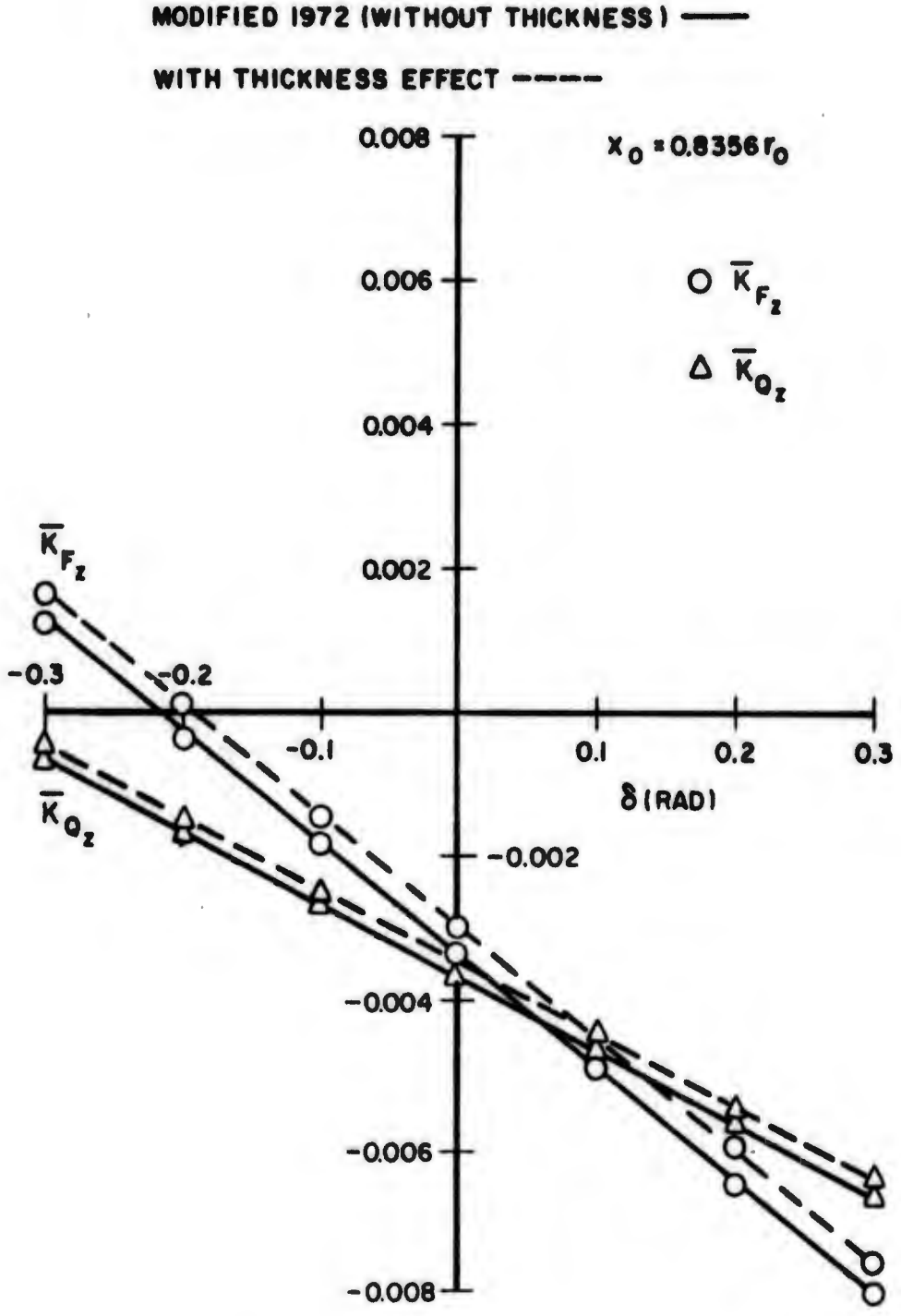

FIG.6. MEAN VERTICAL BEARING FORCE AND BENDING MOMENT COEFFICIENTS ABOUT Z-AXIS VERSUS RUDDER ANGLE δ

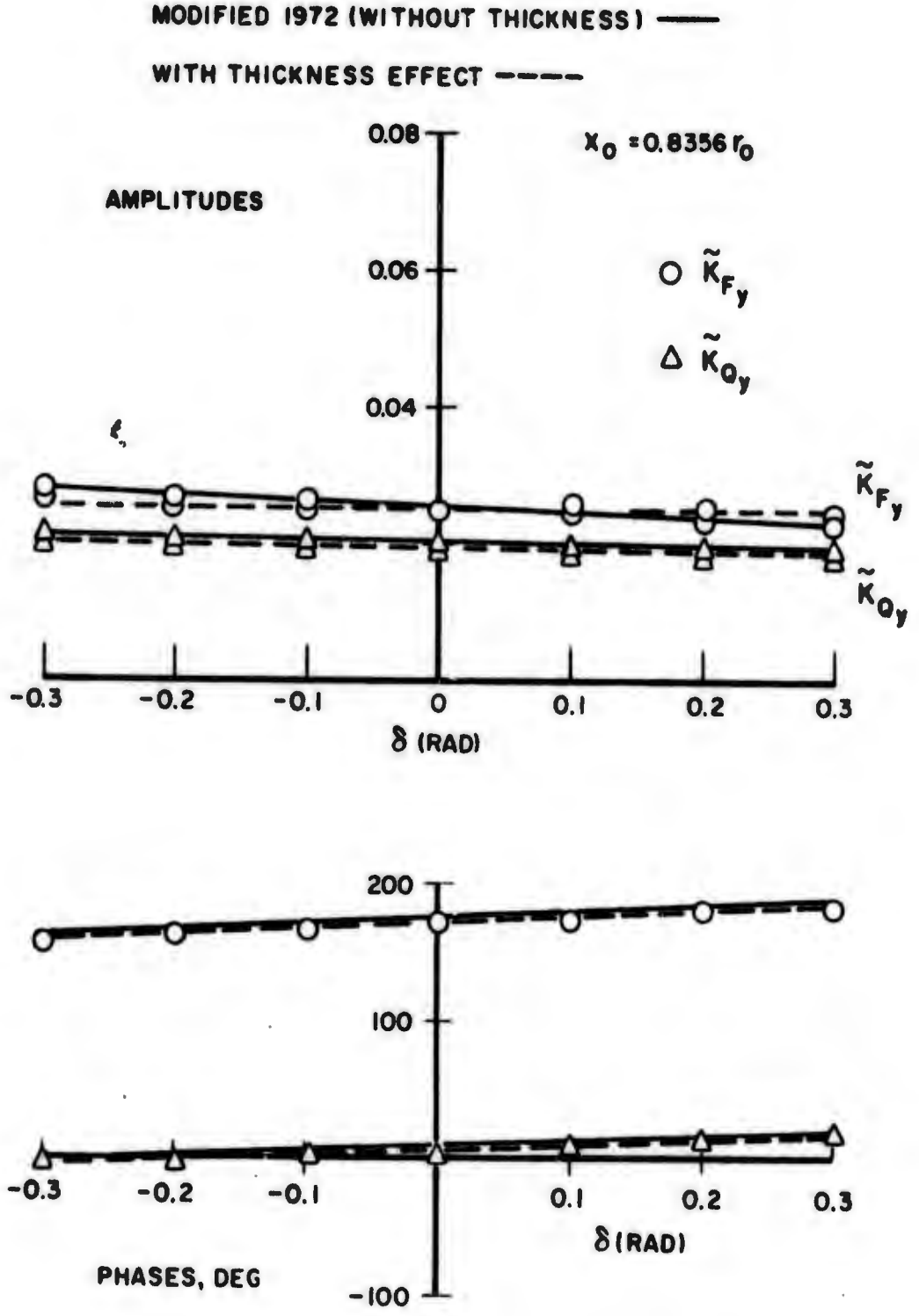

FIG. 7. BLADE-FREQUENCY COEFFICIENTS OF HORIZONTAL BEARING FORCE AND BENDING MOMENT ABOUT Y-AXIS VERSUS RUDDER ANGLE δ

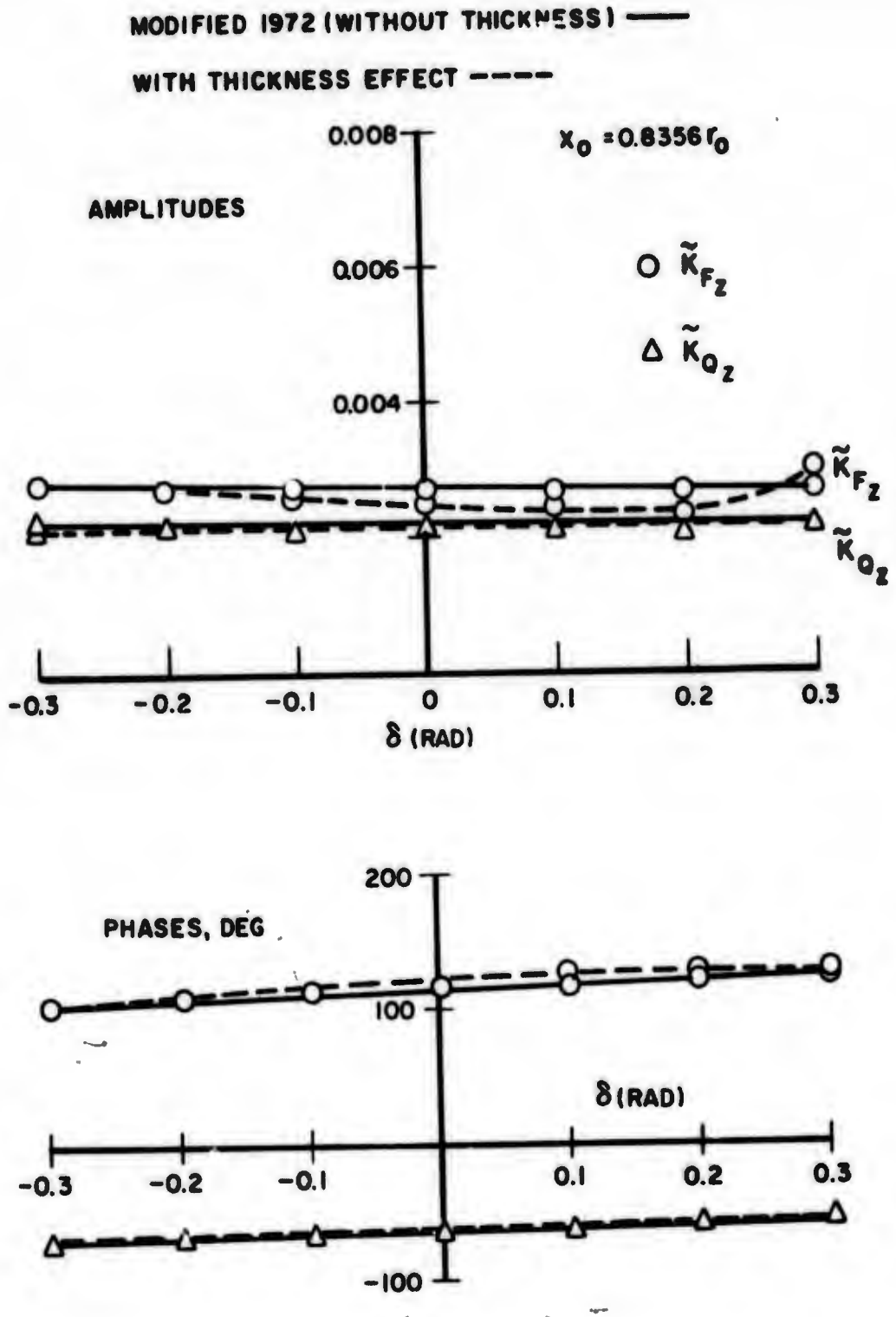

FIG.8. BLADE-FREQUENCY COEFFICIENTS OF VERTICAL BEARING FORCE AND BENDING MOMENT ABOUT Z-AXIS VERSUS RUDDER ANGLE δ

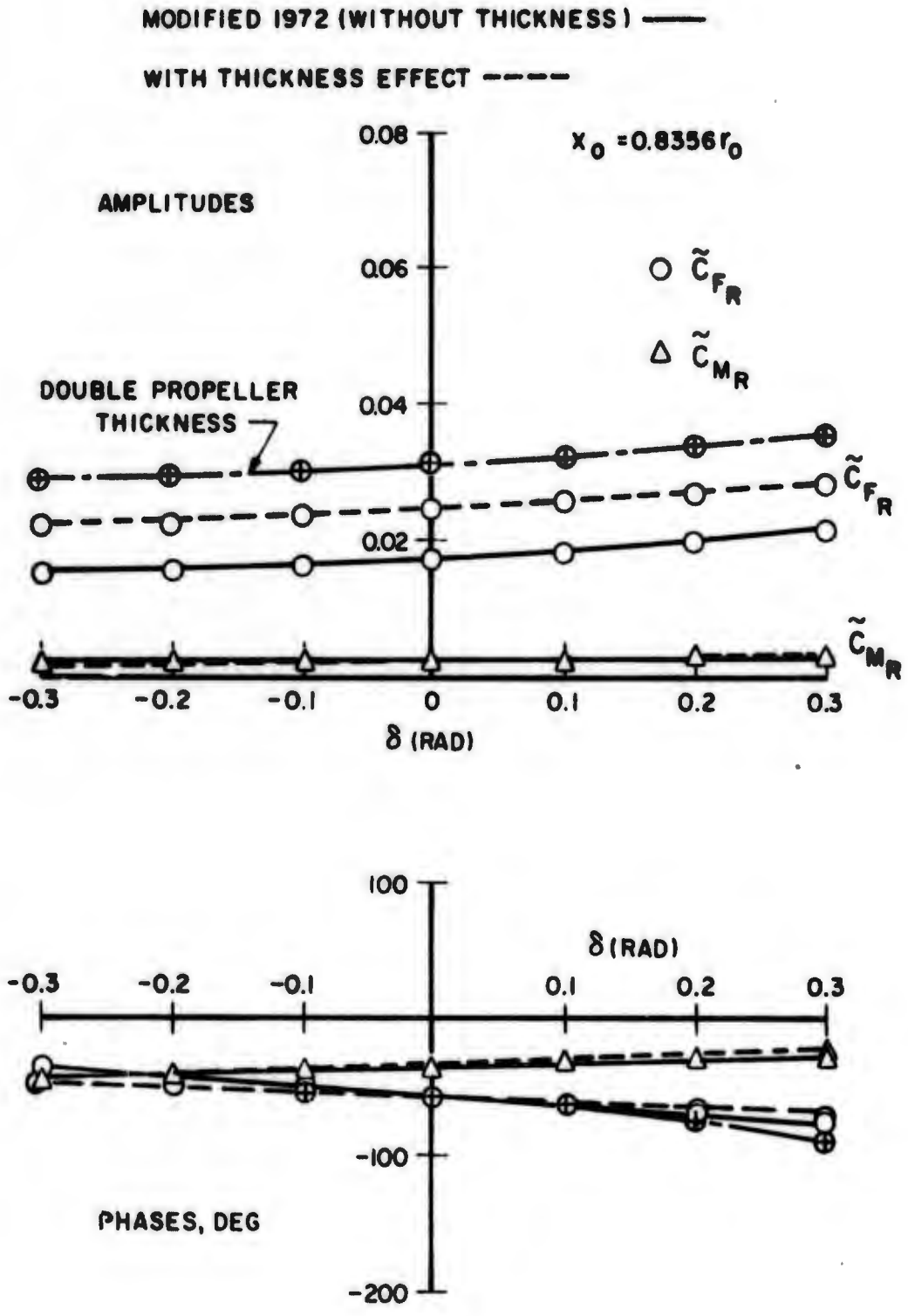

FIG.9. BLADE-FREQUENCY RUDDER LATERAL FORCE AND RUDDER STOCK MOMENT COEFFICIENTS VERSUS RUDDER ANGLE

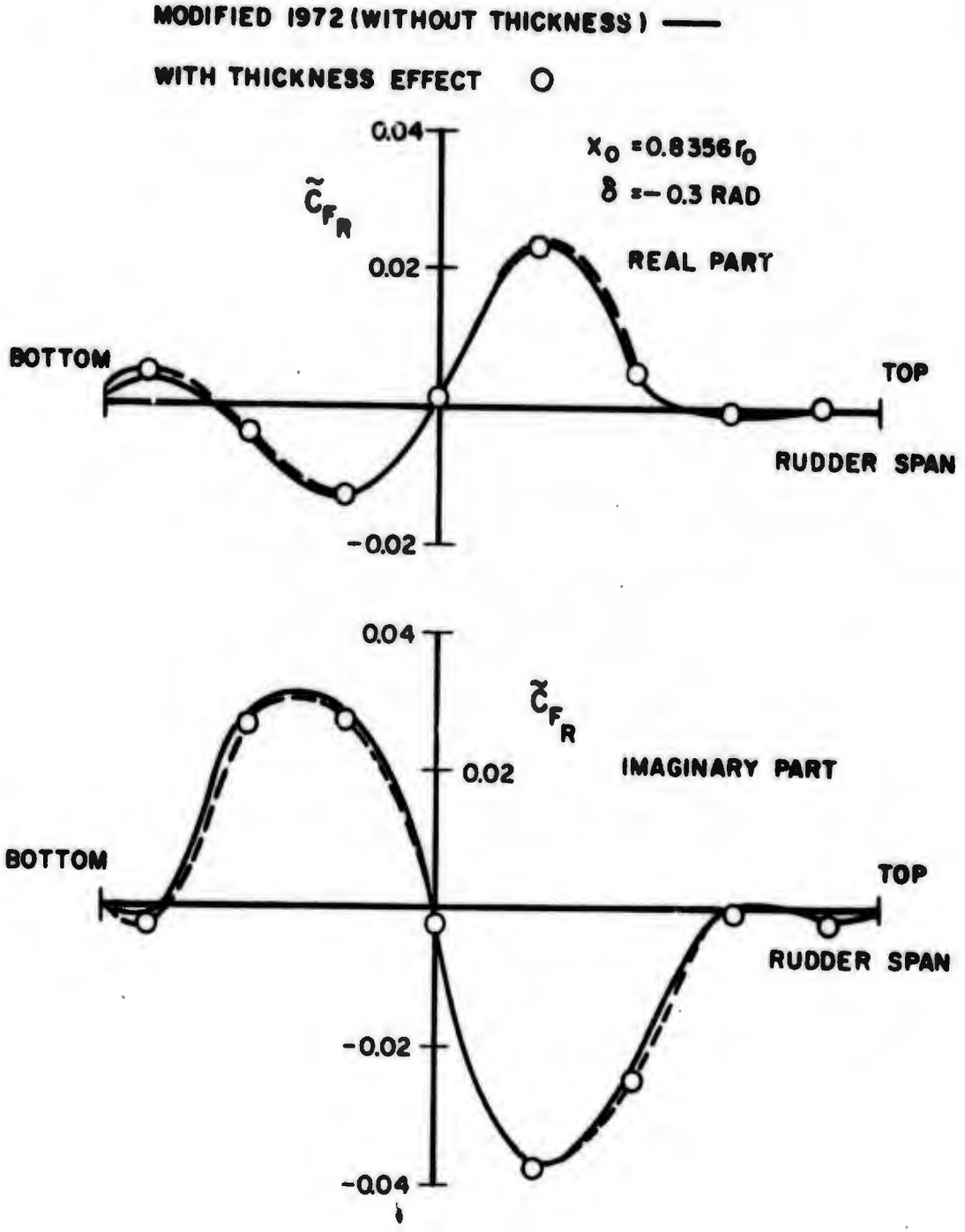

FIG. 10. SPANWISE DISTRIBUTION OF BLADE FREQUENCY $\tilde{C}_{F_R}$ FOR RUDDER ANGLE OF 0.3 RADIAN TO STARBOARD, AND RUDDER LOCATION $X_0 = 0.8356 r_0$

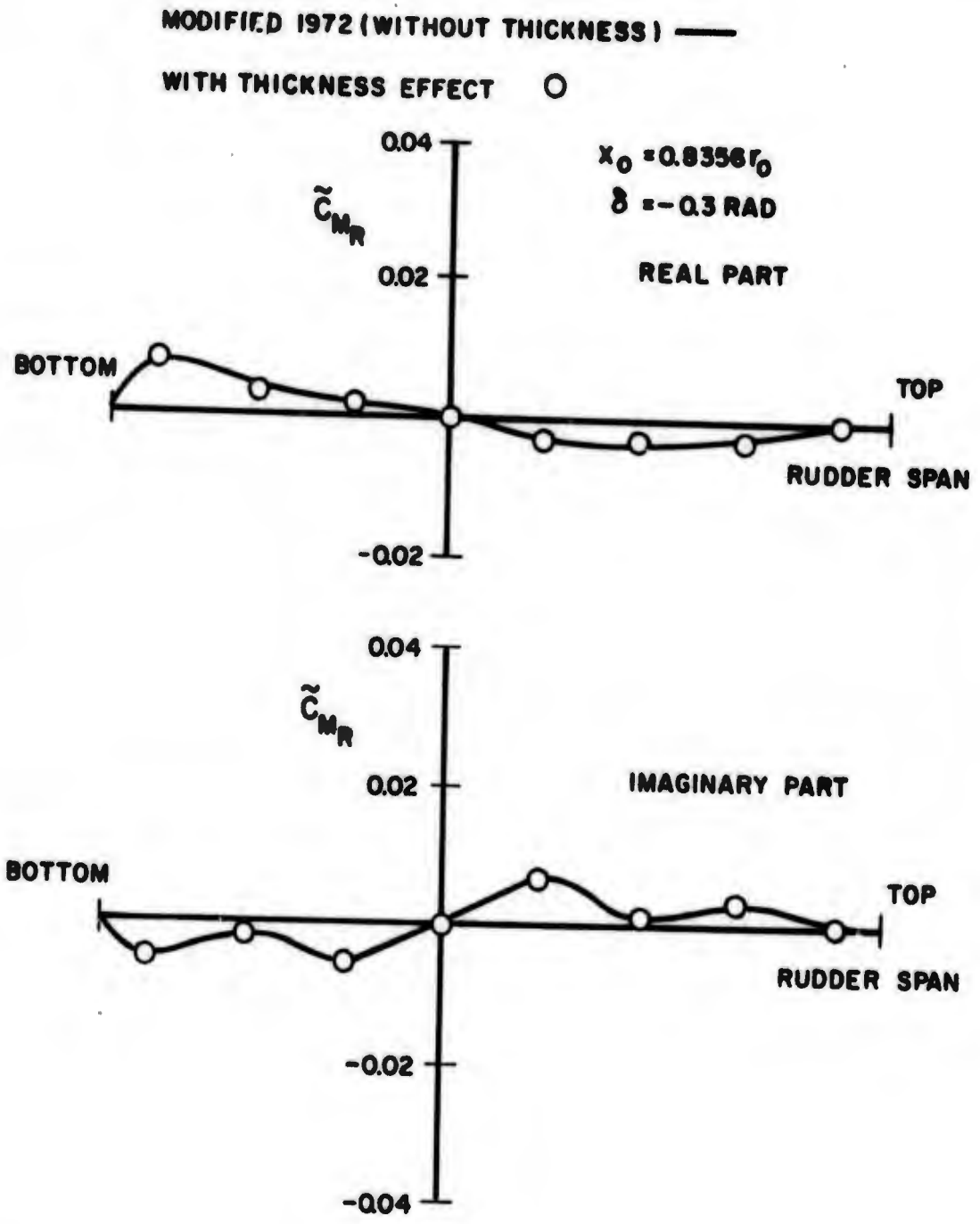

FIG. 11. SPANWISE DISTRIBUTION OF BLADE FREQUENCY $\tilde{C}_{M_R}$ FOR RUDDER ANGLE OF 0.3 RADIAN TO STARBOARD, AND RUDDER LOCATION $X_0 = 0.8356\, r_0$

APPENDIX

The Generalized Lift Operators

Through the expansion scheme for the reciprocal of the Descartes distance R (Equation 17 or Equation 27) the chordwise dependence of the control or field point is separated from its spanwise dependence in such a way as to permit the integration over the chord to be performed analytically by means of the generalized lift operator technique[1,5,7].

The chordwise dependence of the expressions for the onset velocities due to thickness is shown to be of the form $\exp(\pm if\cos\varphi_\alpha)$ which can be expanded in terms of the following orthogonal and complete set of functions $\{\Phi(\bar{m})\}$

$$(1-\cos\varphi_\alpha),\ (1+2\cos\varphi_\alpha),\ \cos 2\varphi_\alpha, \ldots \cos(\bar{m}-1)\varphi_\alpha, \ldots,\ 0 \le \varphi_\alpha \le \pi \qquad \text{(A-1)}$$

in the form

$$e^{\pm if\cos\varphi_\alpha} \equiv J_o(f) + 2\sum_{n=1}^{\infty}(-1)^n J_{2n}(f)\cos 2n\varphi_\alpha \mp 2i \sum_{n=1}^{\infty}(-1)^n J_{2n-1}(f)\cos(2n-1)\varphi_\alpha$$

where $J_n(f)$ are Bessel functions of the first kind. The orthogonality property of $\{\Phi(\bar{m})\}$ dictates operation on left and right-hand sides of Equations (1) and (2) by the following operators

$$\frac{1}{\pi}\int_o^{\pi} \Phi(\bar{m})\{\ \}\, d\varphi_\alpha$$

where $\Phi(1) = 1 - \cos\varphi_\alpha$ (A-2)

$\Phi(2) = 1 + 2\cos\varphi_\alpha$

$\Phi(\bar{m}) = \cos(\bar{m}-1)\varphi_\alpha\ ,\ \bar{m} > 2$

These are termed "generalized lift operators" to conform with the well-known Glauert lift operator ($\bar{m} = 1$) introduced in steady airfoil theory.

With the designation

$$I^{(\bar{m})}(f) = \frac{1}{\pi}\int_0^{\pi} \Phi(\bar{m}) e^{\,if\cos\varphi_\alpha}\, d\varphi \qquad \text{(A-3)}$$

It can be shown that

$$I^{(1)}(f) = J_0(f) - iJ_1(f)$$

$$I^{(2)}(f) = J_0(f) + 2iJ_1(f)$$

$$I^{(\bar{m})}(f) = i^{\bar{m}-1} J_{\bar{m}-1}(f),\ \bar{m} > 2$$

It can be seen that $I^{(\bar{m})}(-f)$ is the complex conjugate of $I^{(\bar{m})}(f)$.